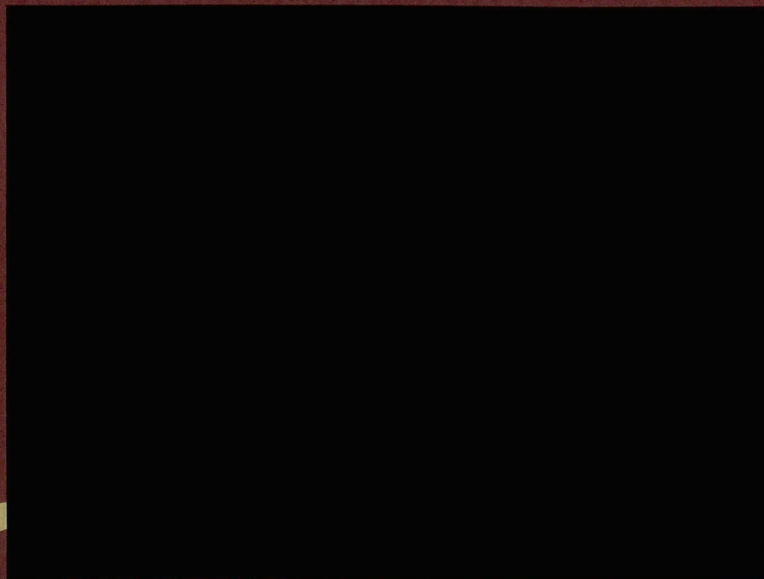

AAR RESEARCH REPORT



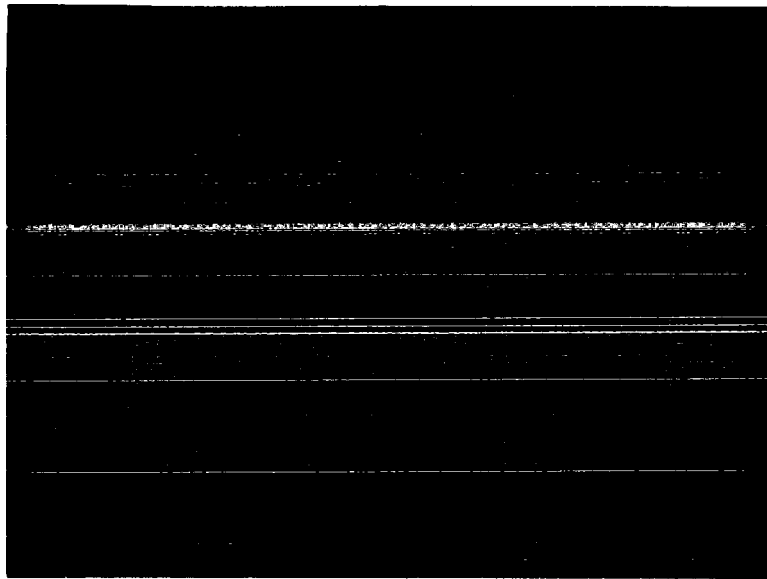
Work performed by:



A SUBSIDIARY OF THE ASSOCIATION OF AMERICAN RAILROADS



1 Dynamics



**VEHICLE/TRACK INTERACTION TESTS
ON THE HEAVY TONNAGE LOOP**

Report No. R-932

**by
Dingqing Li
Lamont Smith**

**Submitted in fulfillment of FRA
Task Order No. 103 DTFR 53-93-C00001**

**Transportation Technology Center, Inc,
a subsidiary of the Association of American Railroads
Pueblo, Colorado
July 1999**

Disclaimer: This report is disseminated by Transportation Technology Center, Inc. (TTCI), a subsidiary of the Association of American Railroads (AAR) for informational purposes only and is given to, and is accepted by, the recipient at the recipient's sole risk. The TTCI/AAR makes no representation or warranties, either expressed or implied, with respect to this report or its contents. The TTCI/AAR assumes no liability to anyone for special, collateral, exemplary, indirect, incidental, consequential, or any other kind of damages resulting from the use or application of this report or its contents. Any attempt to apply the information contained in this report is made at the recipient's own risk.

Copyright©1999 by TRANSPORTATION TECHNOLOGY CENTER, INC., ASSOCIATION OF AMERICAN RAILROADS. All rights reserved.

No part of this publication may be copied or distributed, transmitted, transcribed, stored in a retrieval system, or translated in any language, in any form or by any means, electronic, mechanical, magnetic, manual or otherwise, or disclosed to third parties without the express written permission of the Association of American Railroads.

WORK PERFORMED BY:

REQUEST FOR FEEDBACK



A SUBSIDIARY OF THE ASSOCIATION OF AMERICAN RAILROADS

Report No: **R-932**

Report Title: **Vehicle/Track Interaction Tests on the Heavy Tonnage Loop**

To help us continue to improve the quality and value of AAR reports to our customers, we would appreciate it if you would take a few moments to complete this form. Please feel free to provide further comments in the space below or on additional pages. Thank you for your cooperation.

For each of the following questions, please rate this report on a scale of 1 to 5 where 1 is the lowest rating and 5 is the highest.

Low High
1 2 3 4 5

How important is the subject of the report to your organization?

How effective is the content of the report in assisting your organization address the subject?

How well are the conclusions supported by the research?

How clearly is the report written?

How clearly are the graphics and tables presented and explained?

How would you rate the timeliness of the completion of this project?

If you ordered this report, how promptly was your order processed?

How could this report be improved?

NAME: _____

TITLE: _____

COMPANY: _____

ADDRESS: _____

TELEPHONE: _____ FAX: _____

Please mail or fax the completed form to:
Peggy L. Herman, Assistant Manager-Technology Transfer and Documentation Services,
Transportation Technology Center, Inc., P. O. Box 11130, Pueblo, Colorado 81001
Facsimile Number (719) 584-0716

Next page is blank in original document

1. Report No. R-932	2. Report Date July 1999	3. Period Covered January & June 1998
4. Title and Subtitle Vehicle/Track Interaction Tests on the Heavy Tonnage Loop		
5. Authors Dingqing Li and Lamont Smith		
6. Performing Organization Name and Address Transportation Technology Center, Inc. P.O. Box 11130 Pueblo, CO 81001	7. Type of Report	
9. Sponsoring Agency Name and Address U.S. Department of Transportation Federal Railroad Administration Office of Research and Development 1120 Vermont Avenue, SW Washington, DC 20590	8. Contract or Grant No. DTFR-53-93-C00001	
12. Supplemental Notes	10. Number of Pages 47	
13. Abstract Two vehicle/track interaction tests were conducted by Transportation Technology Center, Inc. (TTCI) at the Facility for Accelerated Service Testing (FAST), Pueblo, Colorado. TTCL, a subsidiary of the Association of American Railroads (AAR), performed the tests on FAST's Heavy Tonnage Loop (HTL) in late January and early June 1998 as part of the FAST/HAL (Heavy Axle Load) program. The overall objectives of the tests included: <ul style="list-style-type: none"> • Measuring 125-ton (HAL) vehicle responses to HTL track geometry conditions • Comparing vehicle responses between a 125-ton vehicle equipped with improved suspension trucks and a 100-ton vehicle equipped with standard suspension trucks • Supporting other FAST/HAL programs <p>These tests included measurements of vehicle responses such as dynamic wheel loads and car body accelerations. The test vehicles were a 125-ton gondola equipped with improved suspension trucks and a 100-ton covered hopper equipped with standard trucks. Track geometry conditions were recorded using two different systems: the new AAR system based on the inertial/laser technology and the EM80 based on rail contacting measurements.</p>	11. Number of References 3	
14. Subject Terms Vehicle/track interaction, heavy axle load, heavy tonnage loop, vehicle responses, track geometry conditions	15. Availability Statement Transportation Technology Center, Inc., a subsidiary of the Association of American Railroads P.O. Box 79780 Baltimore, Maryland 21279-780	

Next page is blank in original document

EXECUTIVE SUMMARY

Two vehicle/track interaction tests were conducted on the Heavy Tonnage Loop (HTL) at the Federal Railroad Administration's (FRA) Facility for Accelerated Service Testing (FAST), Pueblo, Colorado, in late January and early June 1998. The tests were conducted by Transportation Technology Center, Inc. (TTCI), a subsidiary of the Association of American Railroads (AAR), and included measurements of vehicle responses such as wheel loads and car body accelerations. The following test vehicles were used: a 125-ton heavy axle load gondola equipped with improved suspension trucks and a 100-ton covered hopper equipped with standard trucks. Track geometry conditions were recorded using two different systems -- the new AAR system based on the inertial/laser technology and the EM80 that uses rail-contacting measurements. The main conclusions from these two tests are given below.

HAL Wheel Loads

Under nominal FAST train operation conditions, vertical wheel loads were generated mainly between 20 and 60 kips with means of 35 to 45 kips for various HTL sections. Lateral wheel loads were generated mainly between -5 (gage direction) and +15 kips (field direction) with means of -1 to +7 kips for various HTL sections. In curves, lateral wheel loads on both rails were primarily in the field direction indicating lateral vehicle/track interaction in a gage-widening mode.

On the HTL, dynamic wheel loads generated by the 125-ton test car mainly resulted from the lower center roll of the car body. At 40 mph, dynamic vertical loads generated by the 125-ton car were lower (60 to 73 kips) than those (63 to 79 kips) generated by the 100-ton car. This was attributed to the use of the primary suspension pads under the HAL trucks, which might have attenuated higher frequency dynamic force components.

Use of the improved suspension trucks under the 125-ton car led to better steering in the curves (decreased angle of attacks), which in turn led to significantly lower gage-widening loads. For the entire loop, the 125-ton car mean lateral force was 5 kips lower

than that generated by the 100-ton car equipped with standard trucks. For the 6-degree curve, the HAL mean lateral force was 8 kips lower.

In curves, net lateral axle load increased as speed deviated from the balance speed. As speed changed, redistribution of the car weight was not the only reason for the changing lateral wheel loads on the two rails. The axle (truck) steered better when the operation speed was closer to the balance speed, leading to lower net lateral axle loads.

HTL Geometry Conditions

For nearly 100 MGT, the HAL traffic caused insignificant geometry degradation on most HTL track sections. However, the bridge section exhibited higher vertical irregularities. The higher vertical irregularities mainly occurred at the bridge approaches, where track vertical movements (pumping) were observed. The “pumping” action in the approaches may have resulted from rapid track stiffness variation typical of transition zones such as approaches.

On the HTL, lateral geometry variations were mostly in-phase between the two rails; however, this was not the case for vertical geometry variations. Higher lateral geometry deviations (misalignments) measured on one rail were consistently matched by the higher deviations measured on the opposite rail. In addition, the HTL was more variable in the lateral direction than in the vertical direction.

HAL Vehicle Response versus Track Geometry Condition

The tests with two different vehicles indicated that over the same track geometry conditions, vehicles with different characteristics would respond differently. Therefore, relationships between vehicle responses and track geometry conditions are vehicle dependent.

Although the HTL showed higher lateral geometry deviations than vertical deviations, dynamic variations in vertical wheel loads were just as significant as the dynamic variations in lateral wheel loads. Furthermore, unlike geometry parameters, which showed consistent lateral deviations between the two rails, dynamic variations in

lateral wheel loads were not consistent between the two rails. Instead, at 40 mph, the outside rail experienced more variations than the inside rail. In other words, any measured dynamic wheel load was a response due to the excitation of the combined geometry deviations of the two rails, in both the lateral and vertical directions.

The coherence value, that defining the relationship between two signals, was generally low for all cases relating a single geometry parameter as input to a single wheel load as output. This also indicates that any wheel load was not directly related to any single geometry parameter. Relatively, vertical and lateral wheel loads were found to be more related to alignment deviations, with the vehicles responding more to alignment deviations. Use of a cross level parameter (difference of the two vertical profiles) improved coherence values as compared to any single vertical profile, indicating that wheel loads were more related to the cross level parameter than to a single surface parameter.

Next page is blank in original document

Table of Contents

1.0	INTRODUCTION	1
2.0	TEST METHODS	2
2.1	Test Track	2
2.2	Test Vehicles	3
2.3	Vehicle/Track Interaction Measurements	4
2.3.1	Wheel Loads	5
2.3.2	Accelerations	7
2.3.3	Track Geometry Conditions	7
2.4	Test Matrix	9
3.0	TEST RESULTS AND ANALYSES	9
3.1	Distribution of HAL Wheel Loads on HTL	9
3.2	Effects of Train Speed on HAL Wheel Loads	12
3.2.1	Effect on Mean Forces in Curves	12
3.2.2	Dynamic Effects on Wheel Loads	14
3.3	125-ton Vehicle (improved Truck) versus 100-ton Vehicle (Standard Truck)	17
3.3.1	Wheel Loads	17
3.3.2	Accelerations	22
3.4	Relationships between 125-ton Vehicle Responses and Track Geometry Conditions	23
3.4.1	Frequency Content Analyses	24
3.4.2	Coherence Analyses	32
3.4.3	Running Standard Deviations	36
3.5	HTL Geometry Development as Function of Traffic	40
4.0	SUMMARY AND CONCLUSIONS	43
4.1	125-ton Wheel Loads	43
4.2	HTL Geometry Conditions	44
4.3	125-ton Vehicle Response versus Track Geometry Condition	44
	Acknowledgement	46
	References	47

Next page is blank in original document

List of Figures

Figure 1.	Heavy Tonnage Loop (HTL) at TTCi.....	2
Figure 2.	Test Consist Configurations.....	3
Figure 3.	Test Consist Assembled for June 1998 Test	3
Figure 4.	Wheel Sets and their Notations	5
Figure 5.	Test Car with AAR Geometry System.....	8
Figure 6.	Distribution of HAL Wheel Loads on the HTL (40 mph, CCW)	10
Figure 7.	Lateral Wheel Loads in Curved and Tangent Sections (40 mph, CCW)	12
Figure 8.	Mean Values of Wheel Loads for Section 25 (6-degree curve).....	13
Figure 9.	Standard Deviation of Vertical Wheel Loads at Different Speeds	15
Figure 10.	Standard Deviation of Lateral Wheel Loads at Different Speeds.....	16
Figure 11.	Comparison of Wheel Loads Generated by (a) 125-ton Car with Improved Truck (12) and (b) 100-ton Car with Standard Truck (20), 40 mph, CW, Entire Loop	19
Figure 12.	Comparison of Wheel Loads Generated by (a) 125-ton Car with Improved Truck (12) and (b) 100-ton Car with Standard Truck (20) in Curved and Tangent Sections, 40 mph, CW	19
Figure 13.	Frequency Contents of Forces Generated by 125-ton Car and 100-ton Car (40 mph, CW, High Rail).....	21
Figure 14.	Vertical and Lateral Car Body Accelerations Measured at 125-ton Car and 100-ton Car (40 mph, CW).....	23
Figure 15.	Frequency Contents of Vertical Forces under 125-ton Car at Two Speeds.....	25
Figure 16.	Frequency Contents of Lateral Forces under 125-ton Car at Two Speeds.....	26
Figure 17.	Frequency Contents of Vertical Geometry Results (Space Curves) Measured at Two Speeds.....	27
Figure 18.	Frequency Contents of Track Geometry (Space Curves) Measured at Two Speeds.....	28
Figure 19.	Typical Wave Forms of Wheel Loads and Track Geometry (Space Curves) Data, Tangent.....	30
Figure 20.	Typical Wave Forms of Wheel Loads and Track Geometry (Space Curves) Data, 5-degree Curve	31
Figure 21.	Coherence Results between Lateral Track Geometry (Space Curves) and Test Wheel Loads.....	34
Figure 22.	Coherence Results between Vertical Geometry (Space Curves) Data and 125-ton Wheel Loads on High Rail	35

Figure 23. Coherence Results between Cross Level and 125-ton
Wheel Loads on High Rail 35

Figure 24. Running Standard Deviation Results Overlaying
Raw Track Geometry (Space Curves) Data..... 38

Figure 25. Running Standard Deviation Results Overlaying
Raw Data of HAL Wheel Loads 39

Figure 26. Geometry Development with Traffic for Several HTL Sections..... 42

List of Tables

Table 1. HTL Track Configurations 3

Table 2. Modes Contributing to Instrumented Wheel Load Measurements 6

Table 3. Geometry Parameters via New AAR Geometry System and EM80..... 8

Table 4. Test Variables Considered in Each Test..... 9

1.0 INTRODUCTION

Two vehicle/track interaction tests were conducted by the Transportation Technology Center, Inc.'s (TTCI) at the Facility for Accelerated Service Testing (FAST). TTCI, a subsidiary of the Association of American Railroads (AAR), performed the tests on FAST's Heavy Tonnage Loop (HTL) in late January and early June 1998 as part of the FAST/HAL (Heavy Axle Load) program. The overall objectives of the tests included:

- Measuring 125-ton car (HAL vehicle) responses to HTL track geometry conditions
- Comparing vehicle responses between a 125-ton vehicle equipped with improved suspension trucks and a vehicle equipped with standard suspension trucks
- Supporting other FAST programs

The test vehicles included a 125-ton gondola car equipped with improved suspension trucks, and a 100-ton covered hopper car equipped with standard suspension trucks. Measured vehicle responses included wheel/rail forces using instrumented wheel sets, and accelerations at various car locations. The geometry conditions were recorded using the new AAR geometry system. This new geometry system was recently developed and installed under a loaded freight car: the 100-ton covered hopper. It measures track geometry space curves in both lateral and vertical planes, in addition to gage, cross level, curvature, lateral alignment, and vertical profiles or surfaces (alignments and surfaces are based on mid-chord offsets from a 62-foot chord length). In addition, the EM80 geometry car has been used to regularly monitor HTL geometry conditions. However, the EM80 geometry car does not measure track geometry space curves, but utilizes contact measurement of the rails under the car.

This report will discuss the test results addressing the first two objectives listed earlier. Section 2.0 of this report describes the test vehicles and the test methods used for measuring vehicle responses and track geometry conditions. Test variables such as track conditions and truck characteristics will also be given. Section 3.0 discusses the test results and analyses.

These results will include:

- Magnitude distributions of wheel loads due to the 125-ton test car
- Effects of train speed on vehicle response
- Comparison of vehicle responses between the two vehicles equipped with two different types of trucks
- Relationship studies between 125-ton vehicle responses and track geometry conditions
- HTL geometry development as a function of HAL traffic accumulation

Section 4.0 provides final conclusions derived from testing.

2.0 TEST METHODS

2.1 TEST TRACK

The HTL is a 2.7-mile (14,256-foot) track that is divided into many sections for evaluating various track components. Figure 1 shows HTL sections with the various track components present during the two tests. Table 1 lists the curvature, superelevation, and balance speeds for several major sections shown in Figure 1. The HTL test track is maintained as a Class 4 track as defined by the Federal Railroad Administration (FRA) Standards.¹ The nominal train operation speed over the HTL is approximately 40 mph.

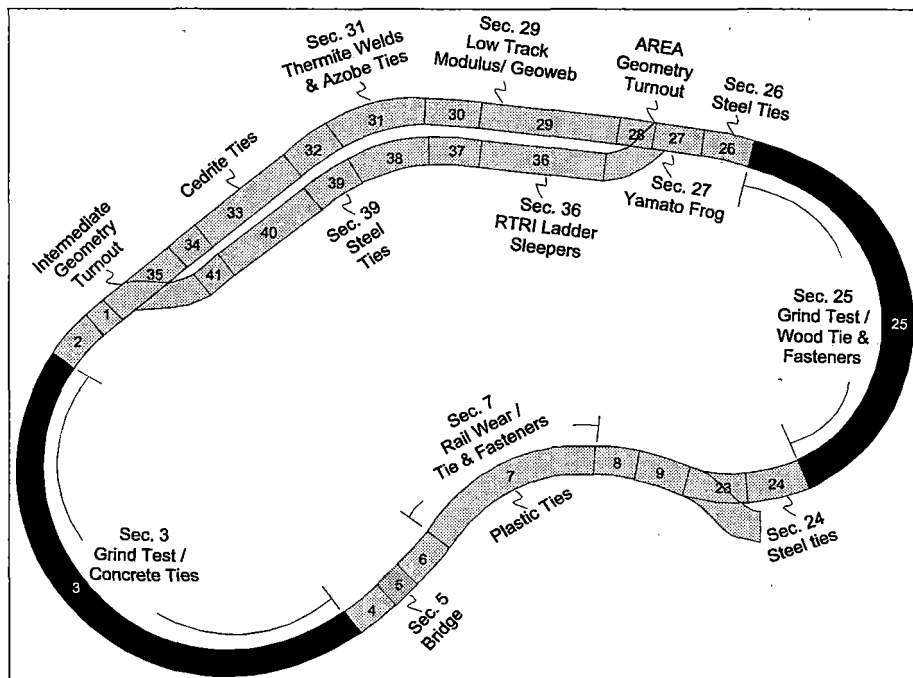


Figure 1. Heavy Tonnage Loop (HTL) at TTCI

Table 1. HTL Track Configurations

Section No.	Curvature Degree	Superelevation (inches)	Balance Speed (mph)
3	5	4	34
5	0	0	-
7	5	4	34
25	6	5	35
29	0	0	-
31	5	4	34
33	0	0	-

2.2 TEST VEHICLES

Separate test consists were assembled for both the late January and early June tests.

Figure 2 illustrates the configurations of these two test consists. Figure 3 is a photo of the second consist.

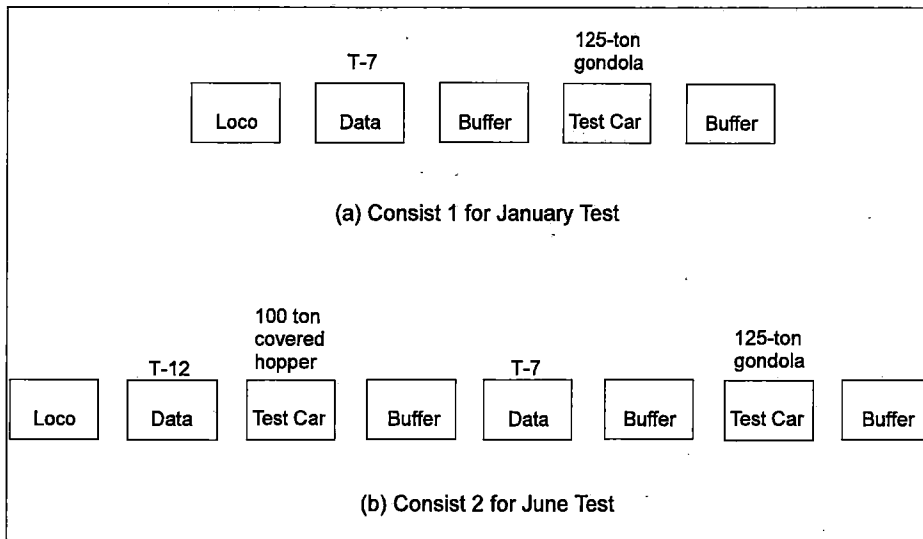


Figure 2. Test Consist Configurations

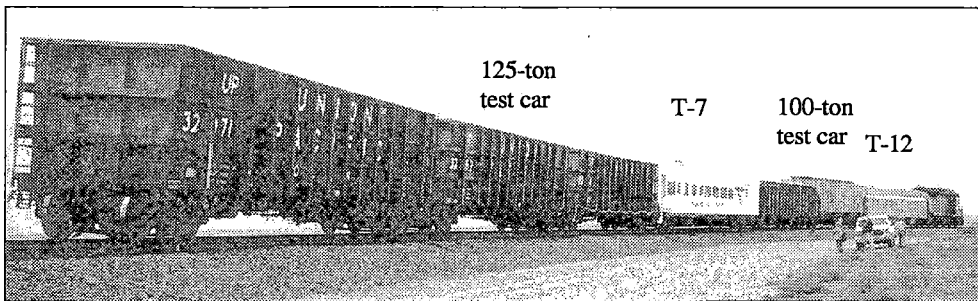


Figure 3. Test Consist Assembled for June 1998 Test

The first test consist (Figure 2a) was used in the late January test. This consist included a data acquisition car (T-7) and a test car (a 125-ton gondola). The test car was equipped with instrumented wheel sets (38-inch wheel diameter) and accelerometers. Two buffer cars were included in the consist in an attempt to better simulate the FAST train operation conditions.

The trucks used under the test car were three-piece trucks with improved suspension characteristics, including diagonal bracing between the side frames to provide truck squaring (warp stiffness) and primary suspension pads.²

The second test consist was used in the June test. As shown in Figure 2b, the second consist included the same 125-ton gondola car used in the first consist, as well as a 100-ton covered hopper as the second test car. Another data acquisition car (T-12) was used to handle the data from the 100-ton test car. Similar to the 125-ton gondola car, this covered hopper was also equipped with instrumented wheel sets (36-inch wheel diameter), accelerometers, and other instrumentation (unrelated to this project). In addition, an inertial/laser based geometry system was installed 28.5 inches ahead of the lead axle.

The trucks used under the 100-ton covered hopper were standard three-piece trucks (ride control with constant damping) without improved suspension characteristics.

2.3 VEHICLE/TRACK INTERACTION MEASUREMENTS

The January test collected only vehicle response data while the June test collected both vehicle responses and track geometry conditions. Geometry data were not collected in the January test because the EM80 car was under repair and the new AAR geometry system was still under development. Nevertheless, the January test was performed to meet the requirements of other FAST test programs.

Vehicle response measurements included wheel loads from the instrumented wheel sets and accelerations of car body, truck, and axle. Track condition measurements

included track geometry and rail friction conditions. The following sections give a more detailed description of each measurement taken.

2.3.1 Wheel Loads

Wheel loads were measured using instrumented wheel sets. For each of the two test vehicles, two wheel sets were installed in the lead truck. Figure 4 shows the notations of instrumented wheels for each test vehicle. For each wheel, the measurements included vertical wheel load (V), lateral wheel load (L), and relative wheel/rail contact position (tread position).

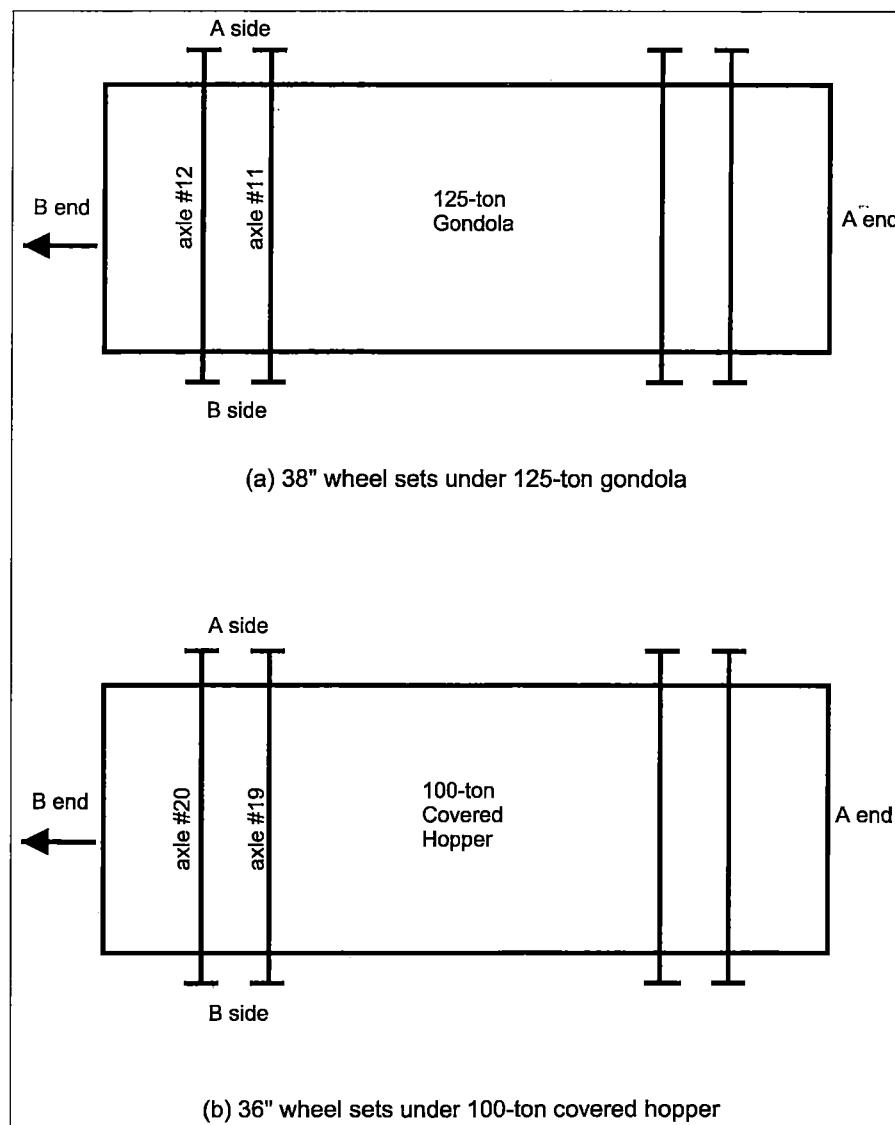


Figure 4. Wheel Sets and their Notations

These wheel sets are defined in terms of axle number and truck side. Facing the direction of travel, A-side is always the right side; whereas, B-side is always the left side. The axle numbers are 11 and 12 for the 125-ton car, and 19 and 20 for the 100-ton car. In this report, labeling of wheel loads will be based on the combinations of force (V or L), side (A or B) and axle number (11, 12, 19, or 20). For example, a label of VA20 will be the vertical wheel load exerted on the right rail (facing the direction of travel) under the lead axle of 100-ton test car.

A positive vertical wheel load corresponds to a downward force applied on the rail. Depending on which rail, a positive lateral wheel load has a different direction but always points away from the center of the track (i.e., in the field direction). A negative lateral wheel load is always a force pointing toward the center of the track (i.e., in the gage direction).

The data was collected at a rate of 500 samples per second. The raw data was filtered at 120 Hz. Within this frequency range, the instrumented wheel sets are expected to provide measurements of wheel loads corresponding to the following vehicle modes:

Table 2. Modes Contributing to Instrumented Wheel Load Measurements

Category	Frequency (Hz)		Mode	Force*
	Loaded	Empty		
Suspension (or rigid car body) modes	0.6 to 1.5	2 to 3	Lower center roll	L, V
	2 to 5	3 to 7	Upper center roll	L, V
	1.5 to 3	2 to 5.5	Yaw	L, V
	2 to 3	3 to 6	Bounce	V
	2.5 to 3.5	4.5 to 7	Pitch	V
Elastic car body modes	5 to 40		Longitudinal torsion, first vertical and lateral bending	L, V

* L = Lateral, V = Vertical

Note: The ranges of resonant frequencies shown above are based only on estimates for 100-125 ton cars

2.3.2 Accelerations

For the 125-ton gondola test car, four accelerometers were used. One vertical accelerometer and one lateral accelerometer were mounted at the center sill over the lead truck. One lateral accelerometer was mounted on the truck, and another lateral accelerometer was mounted on the bearing adapter of the lead axle. For the 100-ton covered hopper, accelerometers were mounted only on the car body. Among those installed, one vertical and one lateral accelerometer was mounted at the center sill over the lead truck similar to the pair mounted on the 125-ton car.

The data was sampled at 500 Hz and filtered at a frequency of 120 Hz. A positive vertical acceleration corresponds to an upward direction. A positive lateral acceleration indicates a right hand acceleration when facing the direction of travel.

2.3.3 Track Geometry Conditions

AAR has recently implemented the geometry measurement system (based on the inertial/laser technology). The system hardware and software was acquired from E. H. Reeves, Inc. The geometry assembly was mounted on the 100-ton covered hopper test car. Figure 5 is a schematic of this test car. As shown, the geometry assembly was installed 28.5 inches ahead of the lead axle of the lead truck. It uses non-contacting sensors to determine rail positions in space; i.e., track geometry space curves, in addition to the regular geometry parameters including superelevation, curvature, gage, lateral alignments, and vertical profiles. Alignment and profile are determined as offsets from a chord 62 feet long:

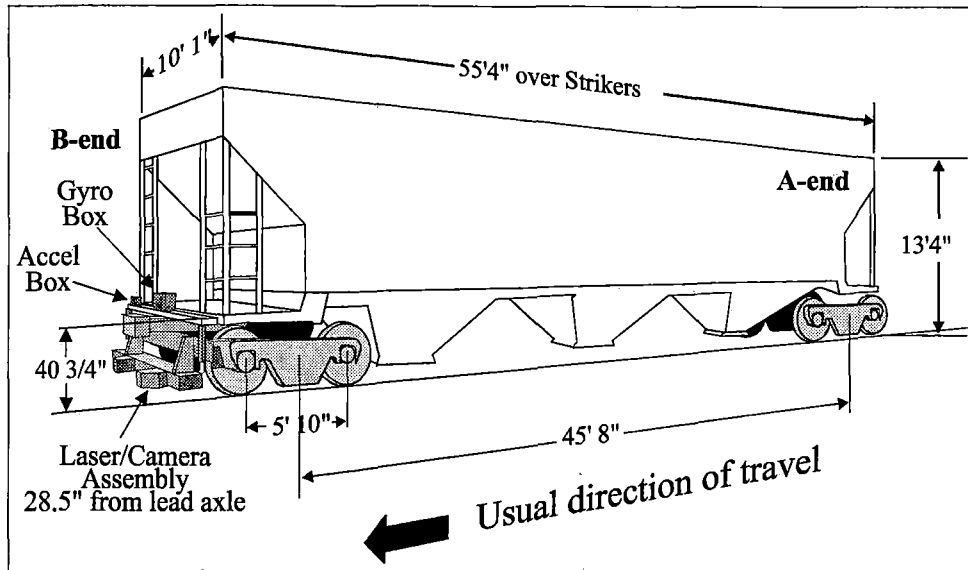


Figure 5. Test Car with AAR Geometry System

Table 3 lists a comparison of those geometry parameters measured by the EM80 car and the new AAR geometry system.

Table 3. Geometry Parameters via New AAR Geometry System and EM80

Track Geometry Parameters	New AAR Geometry System	EM80 Geometry Car
Gage	Yes	Yes
Cross level (or super-elevation)	Yes	Yes
Curvature	Yes	Yes
62-foot chord offsets – alignment left, right	Yes	Yes
62-foot chord offsets – profile left, right	Yes	Yes
Space curves – lateral left, right	Yes	No
Space curves – vertical left, right	Yes	No

The geometry data generated by the new AAR geometry system is actually the distance between a reference and the rail gage face 5/8 inch from top of the rail. This reference represents a line which has removed (filtered) curves having wavelengths larger than 63 feet (however, because of the roll-off effect of the filter, significant signals are still recorded up to wavelengths of approximately 100 feet).

The sampling rate of the AAR geometry system is limited to one sample per foot. Considering that a curve needs at least 3 points to be defined, the shortest wave length the AAR geometry system can measure is 2 feet.

2.4 TEST MATRIX

Table 4 lists the test variables considered in each of these two tests conducted in late January and early June. As shown, these variables included vehicle type, truck type, vehicle speed, travel direction, and track components. For the HTL, the mainline is the loop including Sections 28 through 34, while the bypass is the loop including Section 36 through 41. As already shown in Figure 1 and Table 1, both the mainline and bypass loops include various track components and track curvatures.

Table 4. Test Variables Considered in Each Test

Test Date	Test Car/Truck	Speed (mph)	Direction	HTL
1/28/98	125-ton/improved truck	10, 20, 30, 40	CW, CCW	Mainline, bypass
6/2-6/3/98	125-ton/improved truck, 100-ton/standard truck with geometry system	30, 40, 43	CW, CCW	Mainline, bypass

CW – clockwise, CCW – counterclockwise

3.0 TEST RESULTS AND ANALYSES

3.1 DISTRIBUTIONS OF HAL WHEEL LOADS ON HTL

This section discusses the distributions of HAL wheel loads generated on the HTL under normal operation conditions (i.e., 40 mph, normal rail lubrication). Although lateral and vertical wheel loads were measured for all the wheels under the lead truck, only those under the lead axle are presented unless otherwise specified. In general, the wheel loads (especially lateral wheel loads) under the lead axle have greater influence on vehicle and track performance than those under the trailing axle.

Figure 6 shows distributions over the entire loop of vertical and lateral wheel loads as measured under the 125-ton gondola. These distributions were obtained at a speed of approximately 40 mph traveling in a counterclockwise direction. Note that wheel A

was running on the outside rail relative to the loop whereas wheel B was running on the inside rail.

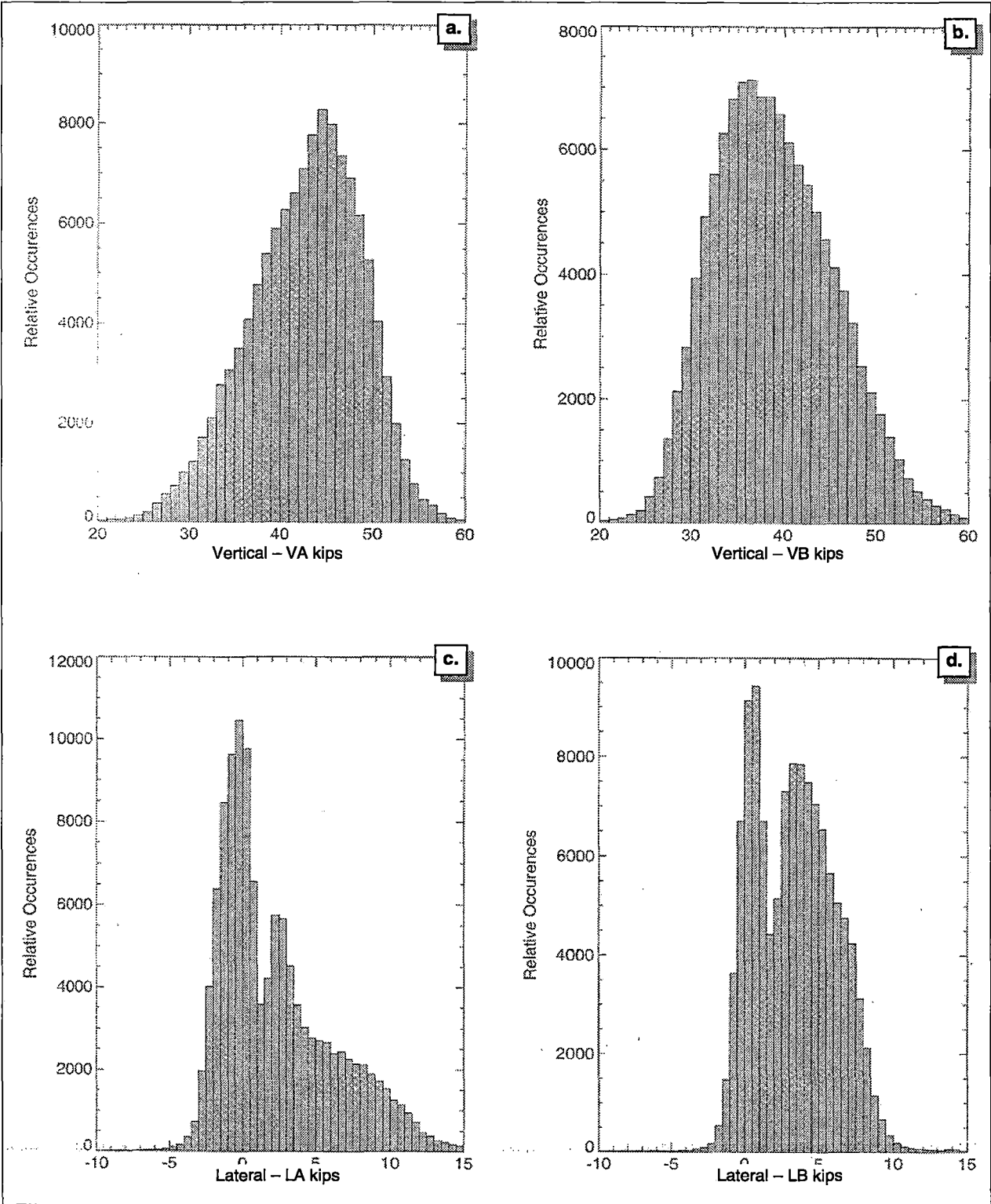


Figure 6. Distribution of HAL Wheel Loads on the HTL (40 mph, CCW)

As shown, the vertical wheel loads ranged mainly between 20 and 60 kips as compared to the nominal static loads of 39 kips. Variations from the nominal static values were due to unbalances in the curves as well as dynamic vehicle/track interactions. Because the train ran at a speed above the balance speeds (Table 1), car weight was shifted more to the outside rail (A wheel) in curves. Consequently, VA can be seen skewed above 39 kips; whereas, VB can be seen skewed lower than 39 kips.

The lateral wheel loads measured ranged mainly between -5 and +15 kips. Again, a positive sign in lateral wheel load denotes a force in the field direction (or flanging lateral force), while a negative sign indicates a force in the gage direction. As can be seen, the outside rail (LA) experienced higher flanging lateral forces at 40 mph than the inside rail (LB). For the inside rail itself, it also experienced more lateral flanging forces than forces in the gage direction. The fact that both rails experienced more and higher lateral flanging forces indicates that the vehicle/track interaction in lateral direction was primarily a gage-widening mode for the HTL track.

Figure 6 also shows that the wheel loads generated for the entire loop were not normally distributed. Instead, their distributions either are skewed or resemble a bi-modal shape. These non-normal distributions were primarily due to non-normal distributions of track configurations within the HTL. One main factor, for example, is the curvature variation. Each curve would lead to a different mean and a different range.

To illustrate the contribution of individual HTL sections to the entire loop distributions, Figure 7 shows the force distributions in two individual sections (LA – wheel load on the outside rail). The figure shows distributions of lateral wheel loads for Section 25 (6-degree curve) and Section 29 (tangent) with respect to the lateral force distributions (LA) shown in Figure 6. A comparison between the loop and sectional distributions indicates that Section 25 was mainly contributing to the second modal

distribution for the entire loop, while Section 29 was mainly contributing to the first mode distribution for the entire loop.

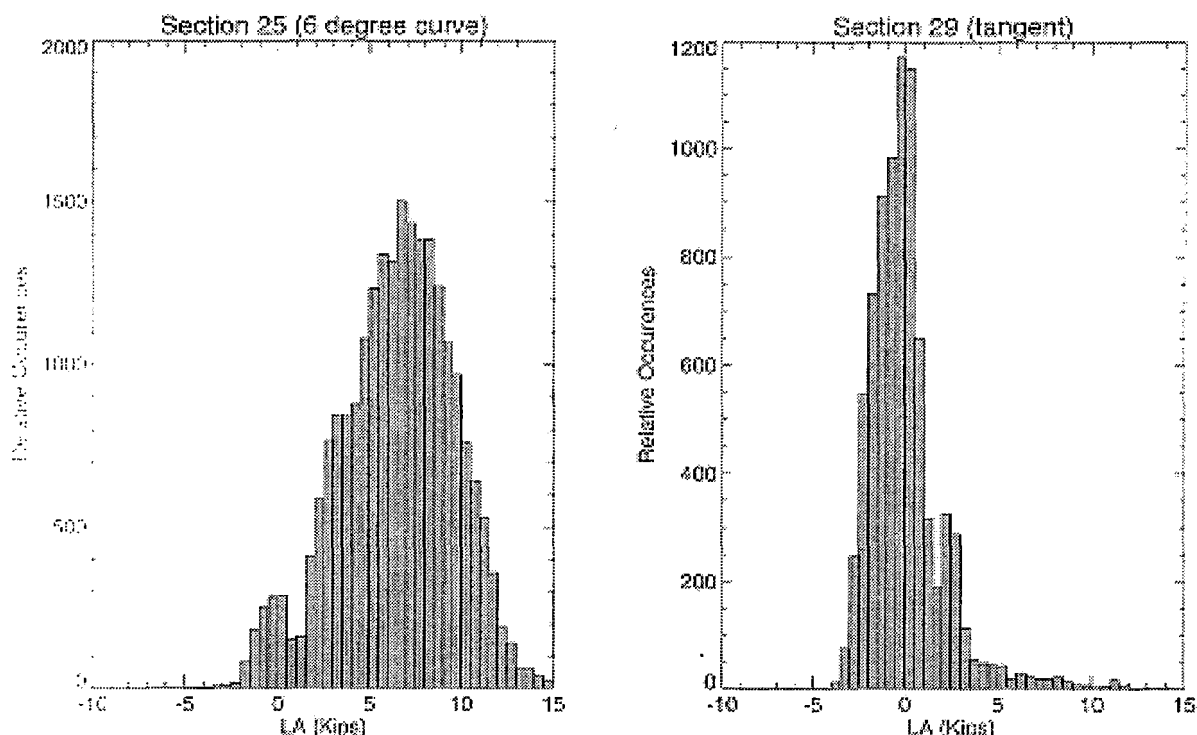


Figure 7. Lateral Wheel Loads in Curved and Tangent Sections (40 mph, CCW)

3.2 EFFECTS OF TRAIN SPEED ON HAL WHEEL LOADS

Tests were conducted at several different speeds to examine the effects of speed on 125-ton car wheel loads. Train speed was expected to have effects from two aspects: the effect on the means of wheel forces in a curve, and the effect on dynamic force variations.

3.2.1 Effect on Mean Forces in Curves

When a train runs at a balance speed in a curve, the car weight should be uniformly distributed between two rails. Unbalanced wheel loads result from speed variations about the balance speed. This effect can be seen in Figure 8, where the measured mean values of both vertical and lateral wheel loads (wheel A was on the high rail) in a 6-degree curve (Section 25) are illustrated.

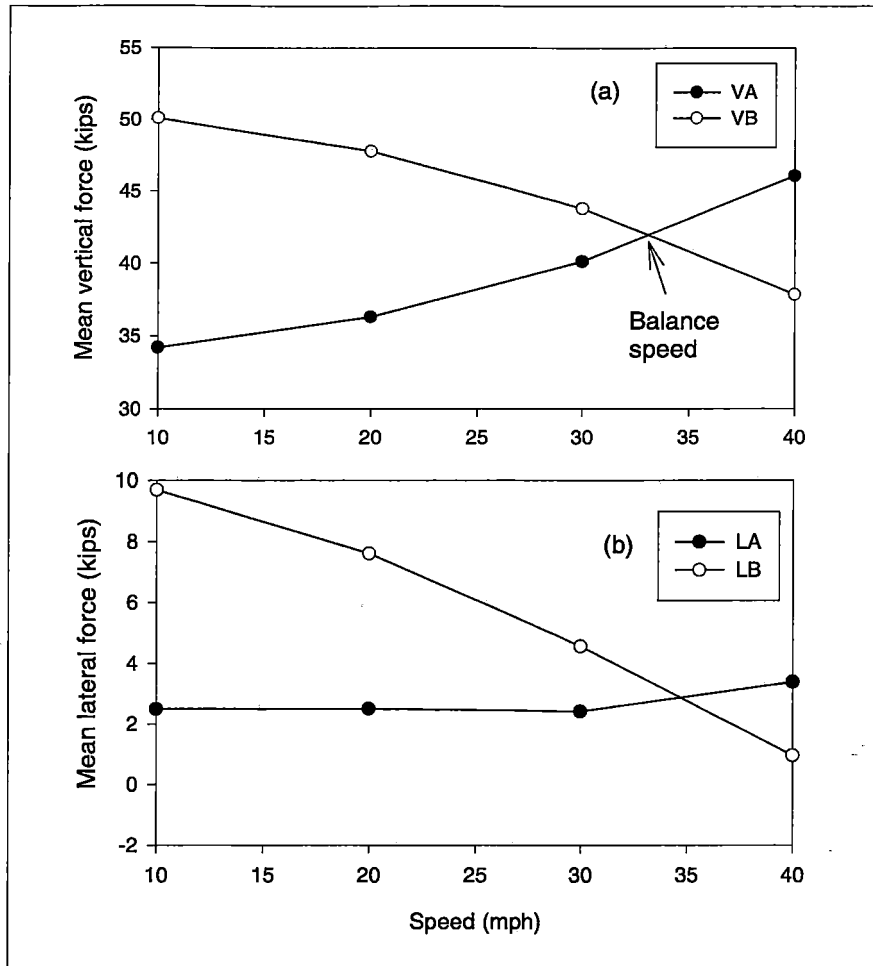


Figure 8. Mean Values of Wheel Loads for Section 25 (6-degree curve)

Figure 8a shows that as speed increased from 10 to 40 mph, vertical wheel loads (mean) shifted to the outside rail (A wheel). However, the average of two means remained the same, regardless of speed. The balance speed on this curve (125-ton gondola) is determined to be approximately 33 mph. At this speed, the mean values of vertical wheel loads on both rails became the same.

Figure 8b shows the effect of speed on lateral wheel loads. Again, as speed increased from 10 to 40 mph, lateral wheel load exerted on the inside rail decreased while the lateral wheel load exerted on the outside rail increased. However, unlike vertical wheel loads, the average of lateral wheel loads on the two rails did not remain the same as speed changed. The further the speed was away from the balance speed, the higher the average of the two mean lateral wheel loads.

The difference between LA and LB is net lateral axle load. Therefore, as speed changed, net lateral axle load increased as speed deviated further from the balance speed. Obviously, as speed changed, redistribution of the car weight was not the only reason for the changing lateral wheel loads on the two rails. It is speculated that axle steering (angle of attack) might also have changed as speed changed. It may have happened that the closer the speed was to the balance speed, the better steering the axle (truck) might have (less angle of attack); therefore, the lower net lateral axle load.

As also shown in Figure 8b, at any speed, the mean of lateral wheel loads on both rails was not zero. Both rails experienced mean flanging forces. As speed increased, the flanging force on the inside rail decreased, while the flanging force on the outside rail increased. However, the increase of lateral flanging force on the outside rail was much smaller than the decrease of flanging force on the inside rail.

Similar trends to those shown in Figure 8 (for Section 25) were also evident in results obtained for other curved sections on the HTL.

3.2.2 Dynamic Effects on Wheel Loads

In this report, force variations due to dynamic vehicle/track interaction are described in terms of the standard deviation (STD) of the measured forces. For the same track section, a higher standard deviation of any force should indicate a higher dynamic variation due to vehicle/track interaction.

Figures 9 and 10 show the effect of speed on vertical and lateral wheel load variations for the four wheels measured in two HTL sections (a tangent and a 6-degree curve). As shown, an increase in speed led to an increase in dynamic force variation for all the wheels.

As expected, the relationships between dynamic variation and speed were non-linear for both vertical and lateral forces. As shown in Figures 9 and 10, the rate of dynamic variation was higher as speed increased.

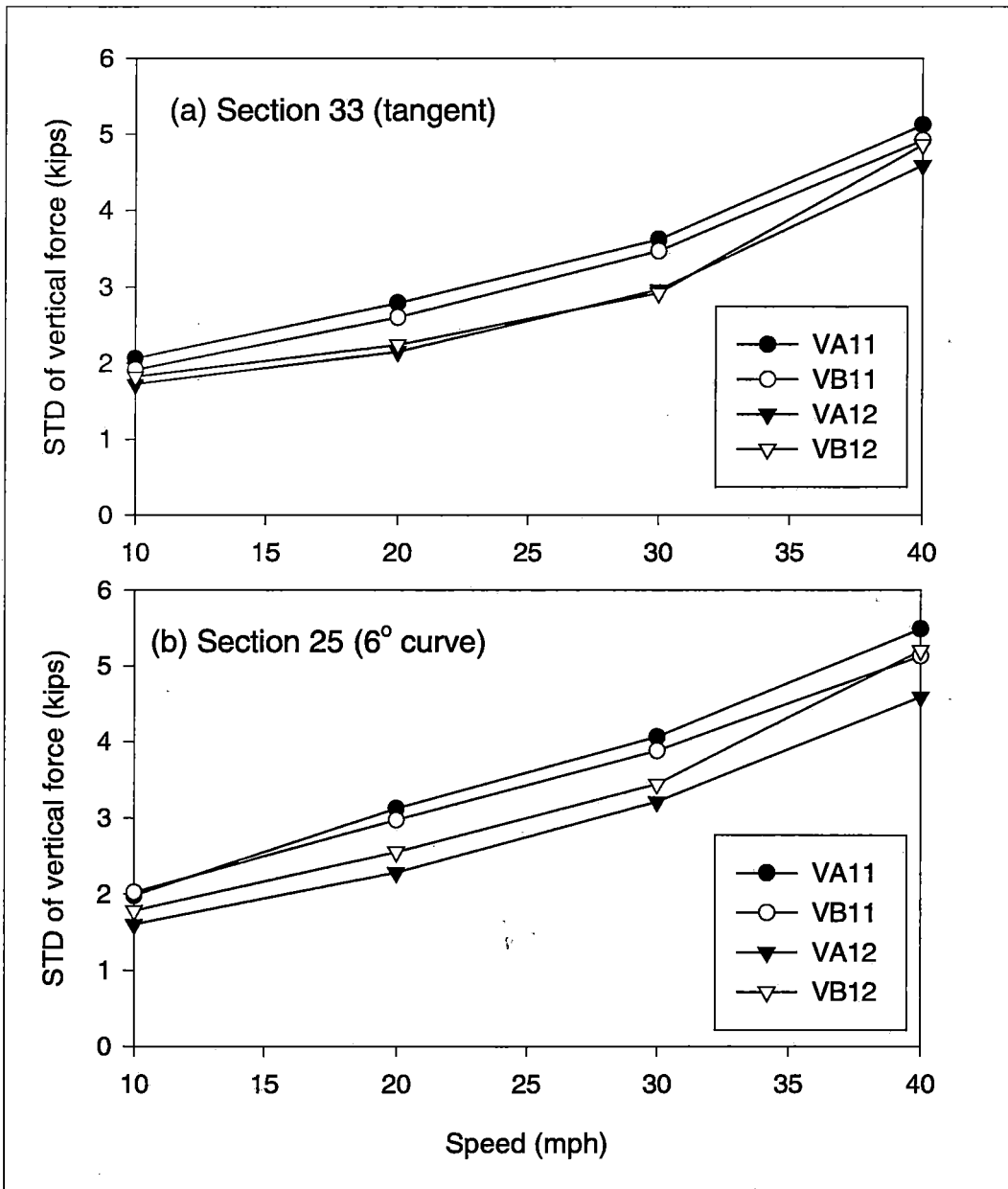


Figure 9. Standard Deviation of Vertical Wheel Loads at Different Speeds

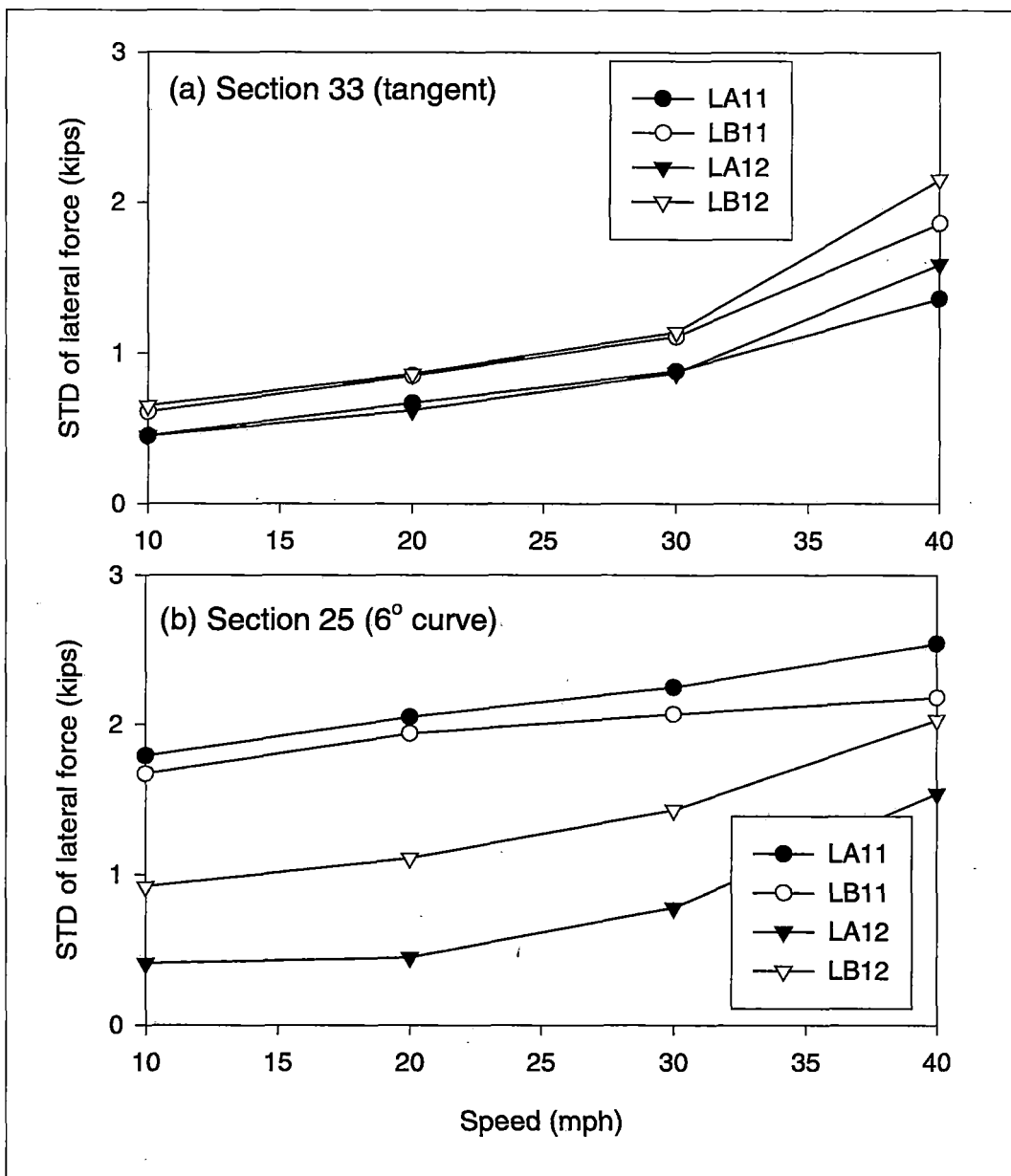


Figure 10. Standard Deviation of Lateral Wheel Loads at Different Speeds

3.3 125-TON VEHICLE (IMPROVED TRUCK) VERSUS 100-TON VEHICLE (STANDARD TRUCK)

During the June test, the consist included two test vehicles. One was the 125-ton gondola equipped with improved trucks; the other was the 100-ton covered hopper equipped with standard trucks. As discussed earlier, the improved trucks have enhancements in their primary suspensions, as well as in truck warp stiffness.

This section compares vehicle responses between these two vehicles. To provide a more complete comparison, vehicle responses including wheel loads and accelerations are discussed both in time domain and in frequency domain.

The two test vehicles were arranged in the same consist (Figure 2b). Therefore, any difference in vehicle response between these two vehicles resulted mainly from the difference in their characteristics, not from train operations and track conditions.

The results shown in this section were obtained from a test run in a clockwise direction at a nominal speed of 40 mph.

3.3.1 Wheel Loads

Figures 11 and 12 show comparisons of the measured wheel load distributions for the entire loop as well as for two representative sections (tangent Section 29 and 6-degree curve Section 25). Note that axle 12 was associated with the 125-ton car equipped with improved suspension trucks and axle 20 was associated with the 100-ton car equipped with standard trucks.

As expected, the 125-ton gondola car generated higher vertical wheel loads than the 100-ton covered hopper for 99.9 percent of the measured forces. This is shown in Figure 11a (Gaussian scale is used for the vertical axis). However, for a small percentage (0.1 percent), the 100-ton covered hopper actually produced higher dynamic vertical loads (ranging 63 to 79 kips) than the 125-ton car (60 to 73 kips). Lower dynamic vertical loads (in the high range) under the 125-ton car might have resulted from the primary

suspension pad, which may attenuate vertical forces at higher frequency ranges as discussed in analyzing the data presented in Figure 13.

Because the test consist was running clockwise above the balance speeds for all the HTL curves, higher vertical wheel loads should have been generated on the outside rail (i.e., wheels B) than on the inside rail. In Figure 11a, this is evident for the 125-ton car, but not so for the 100-ton covered hopper. In fact, the 100-ton car had a twisted car body that led to uneven weight distribution among all the wheels. The resulting uneven distribution between the two wheels of the lead axle is illustrated in Figure 12a for tangent Section 29. As shown in this figure, wheel A consistently measured higher vertical loads than wheel B for the 100-ton car. The difference was roughly 7 kips. At the median, the vertical wheel load was 29 kips for wheel B, and 36 kips for wheel A. In contrast, the vertical loads of the A and B wheels for the 125-ton car were much closer (also illustrated in Figure 12a).

Going back to Figure 11b, the comparison in lateral wheel loads between these two vehicles is shown for the entire loop. As can be seen, the flanging wheel (B wheels) forces (with positive sign) were significantly higher under the 100-ton covered hopper than under the 125-ton car. The difference at the median was approximately 5 kips. However, the lateral wheel loads in the gage direction (negative sign) between these two vehicles were close.

The higher lateral wheel loads generated by the 100-ton covered hopper as compared to the 125-ton car were even more obvious in the 6-degree curve of Section 25 (Figure 12b). The difference in median lateral loads was roughly 8 kips between the two vehicles.

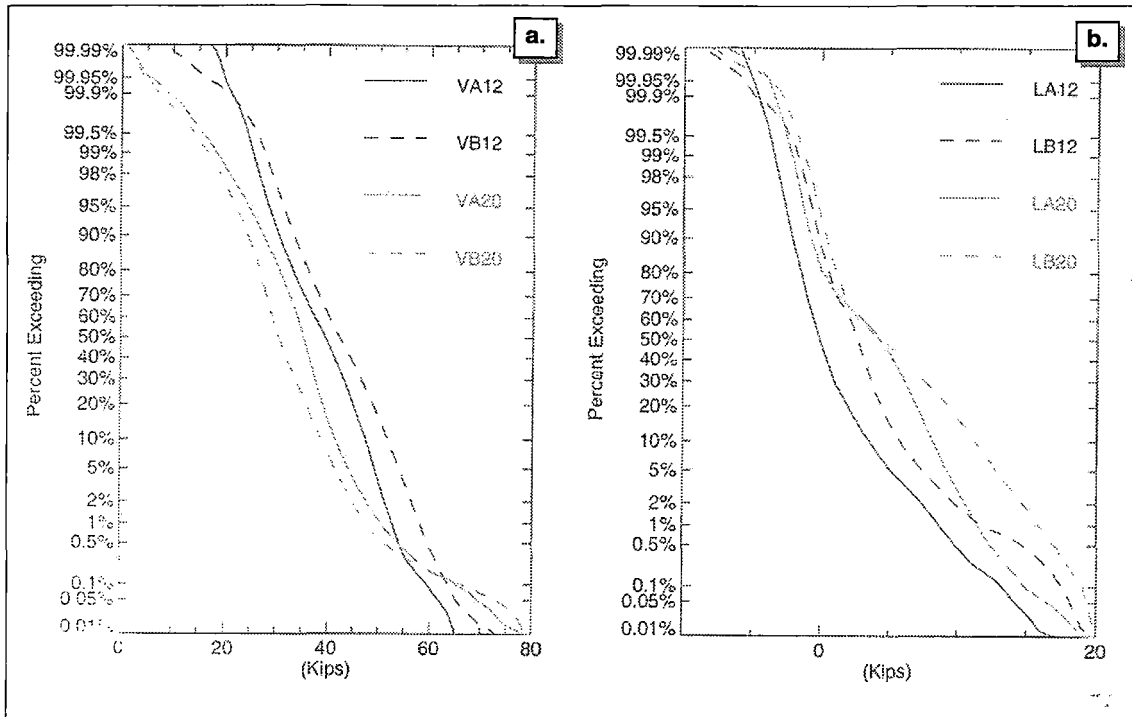


Figure 11. Comparison of Wheel Loads Generated by (a)125-ton Car with Improved Truck (12) and (b)100-ton Car with Standard Truck (20), 40 mph, CW, Entire Loop

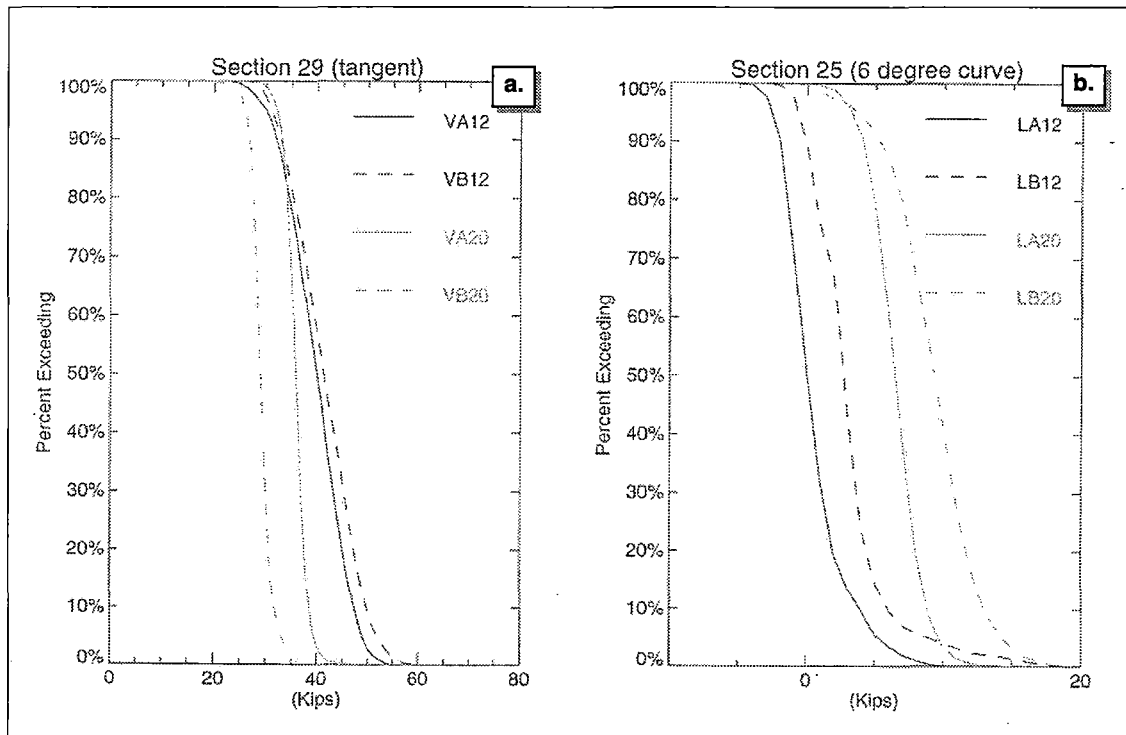


Figure 12. Comparisons of Wheel Loads under (a)125-ton Car with Improved Truck (12) and (b)100-ton car with Standard Truck (20) in Curved and Tangent Sections, 40 mph, CW

The lower lateral wheel forces generated by the 125-ton car resulted mainly from the use of the improved trucks. As reported by the earlier AAR research,² the increased truck warp stiffness (or better truck squaring) along with primary suspension pads has led to much better truck steering in curves (lower angle of attack); and as a consequence, much lower lateral wheel forces.

Figure 13 shows force comparisons in frequency domain (PSD results) between these two vehicles. As can be seen, the vertical wheel load generated under the 125-ton car is primarily concentrated at two frequencies (1.1 and 6 Hz). In contrast, the vertical force generated under the 100-ton covered hopper had energy distributions across a much wider spectrum. For the 125-ton car, use of the primary suspension pad in the improved suspension trucks may have attenuated vertical forces at higher frequencies.

The frequency distribution of lateral force for the 100-ton covered hopper shows a pattern similar to that under the 125-ton car, although the covered hopper still generated lateral forces across a wider frequency range.

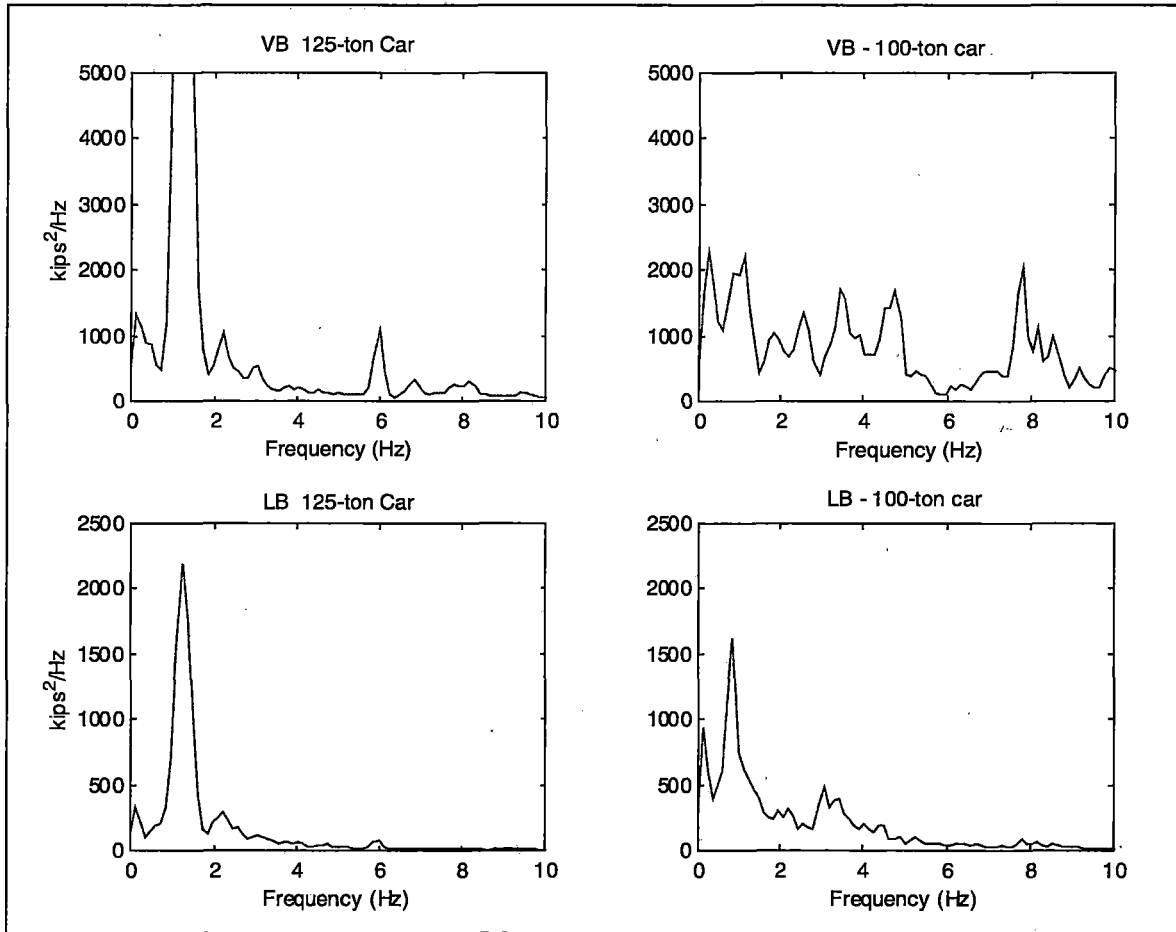


Figure 13. Frequency Contents of Forces Generated by 125-ton Car and 100-ton Car (40 mph, CW, High Rail)

3.3.2 Accelerations

As mentioned earlier, several accelerometers were installed on both test vehicles.

Accelerometers, one in the vertical and one in the lateral direction were installed at the center sill (directly above the trucks) of the car body for each vehicle. However, direct magnitude comparisons of acceleration results may not be completely justified between these two vehicles. This is because acceleration measurements (especially due to roll movements) are sensitive to accelerometer location relative to the roll. The accelerometer locations at the center sills were somewhat inconsistent between these two vehicles.

Unlike the instrumented wheel sets, the accelerometers were sensitive to vehicle responses not only at lower rigid modes, but also at higher flexible car-body modes. Significant noise at higher frequencies could also contribute to acceleration measurements. For this reason, all the acceleration signals were filtered at 10 Hz during the post data reduction. This cut-off frequency is based on the FRA safety standards.¹

Figure 14 shows the distributions of vertical and lateral accelerations for the two test vehicles. For both vehicles over the entire loop, vertical accelerations ranged from -0.2g to 0.2g, and lateral accelerations ranged from -0.1g to 0.3g. Note that positive direction for vertical acceleration is upward, and positive direction for lateral acceleration is toward right when facing the direction of travel.

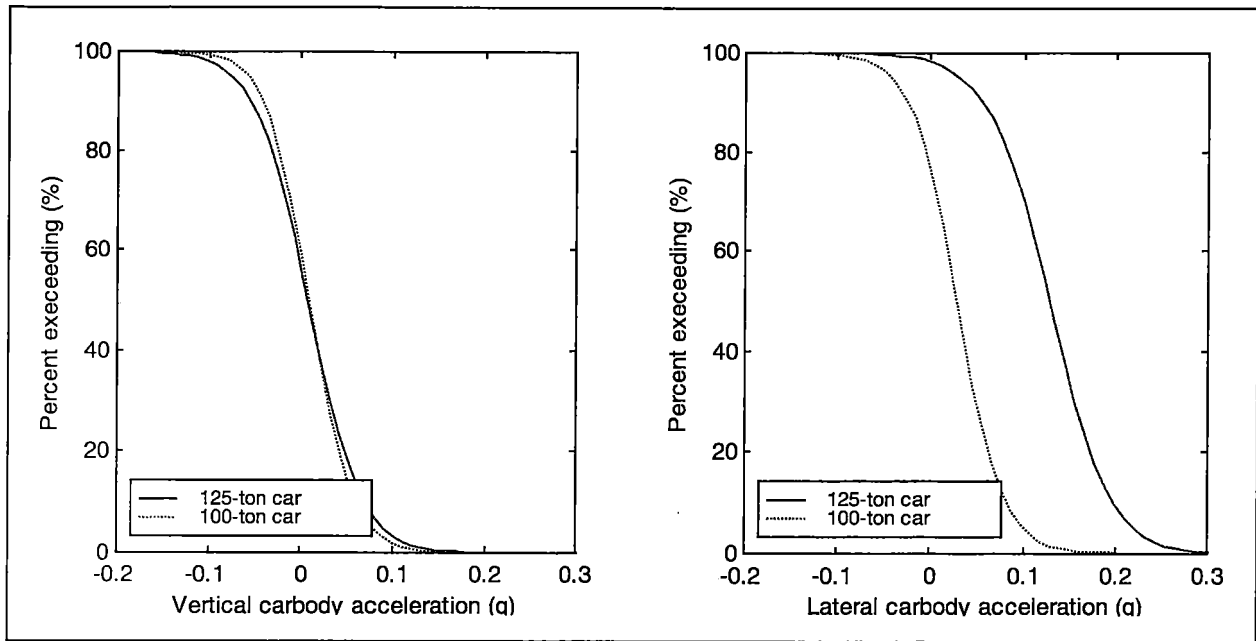


Figure 14. Vertical and lateral Car Body Accelerations Measured at 125-ton Car and 100-ton Car, (40 mph, CW)

3.4 RELATIONSHIPS BETWEEN 125-TON VEHICLE RESPONSES AND TRACK GEOMETRY CONDITIONS

The June test provided data to study vehicle responses to track geometry conditions. However, it needs to be realized from the beginning that although vehicle responses are related to track geometry inputs, their relationships cannot be unique. They are subject to influences from other factors such as vehicle type and characteristics, train speeds, wheel and rail profiles, and rail lubrication conditions.

In this report, the characterization of track geometry conditions used (space curves) do not miss “blind frequencies” as mid-chord offsets may do. The vertical and lateral wheel loads measured under the first axle of the 125-ton gondola are used to characterize vehicle responses to track geometry. Therefore, the relationships between vehicle responses and track geometry conditions are those between measured wheel loads and track geometry space curves. To reduce the influence of other factors, these relationships are determined from the same test runs with the same test consist measuring both the vehicle response and track geometry conditions simultaneously.

3.4.1 Frequency Content Analyses

This section discusses frequency content distributions for track geometry and wheel loads; i.e., the power spectrum density (PSD) results. To better illustrate the possible causes for major energy concentrations, PSD results were obtained for two test runs at two different speeds: i.e., at approximately 30 and 43 mph. Both runs were conducted in a clockwise direction around the loop, passing through the bypass.

Frequency content results (or PSD results) are often used to show the frequency range in which a measured event (a wheel load or geometry parameter) is concentrating its energy. For track geometry, however, spatial frequency (or wavelength) is used more often to represent their frequency contents. However, to be consistent, only time frequency is used in the following PSD results. Time frequency can be determined based on spatial frequency through multiplying by train speed.

Wheel Loads

Figures 15 and 16 show the PSD results of vertical and lateral wheel loads measured under the 125-ton car. The results are shown for two different speeds (30 mph and 43 mph). As shown, regardless of speed and load direction, the first major peak was at approximately 1.1-1.2 Hz. Since this frequency was not influenced by speed, it is considered to correspond to one of the car body rigid modes. Because this peak occurred at the same frequency for both vertical and lateral wheel loads, it is most likely that this frequency was the resonant frequency for the car-body lower center roll or yaw mode. Since much larger dynamic response was measured in the vertical direction than in the lateral direction, lower center roll was considered the most like mode. In fact, the time histories of either vertical wheel loads or lateral wheel loads were mostly out of phase between the two rails, characteristic of wheel loads due to car body roll (see later waveform comparisons in Figures 19 and 20).

For the vertical wheel loads shown in Figure 15, the energy level at the first peak increased as speed increased. Dynamic response in the vertical direction at this resonant frequency was higher at higher speeds.

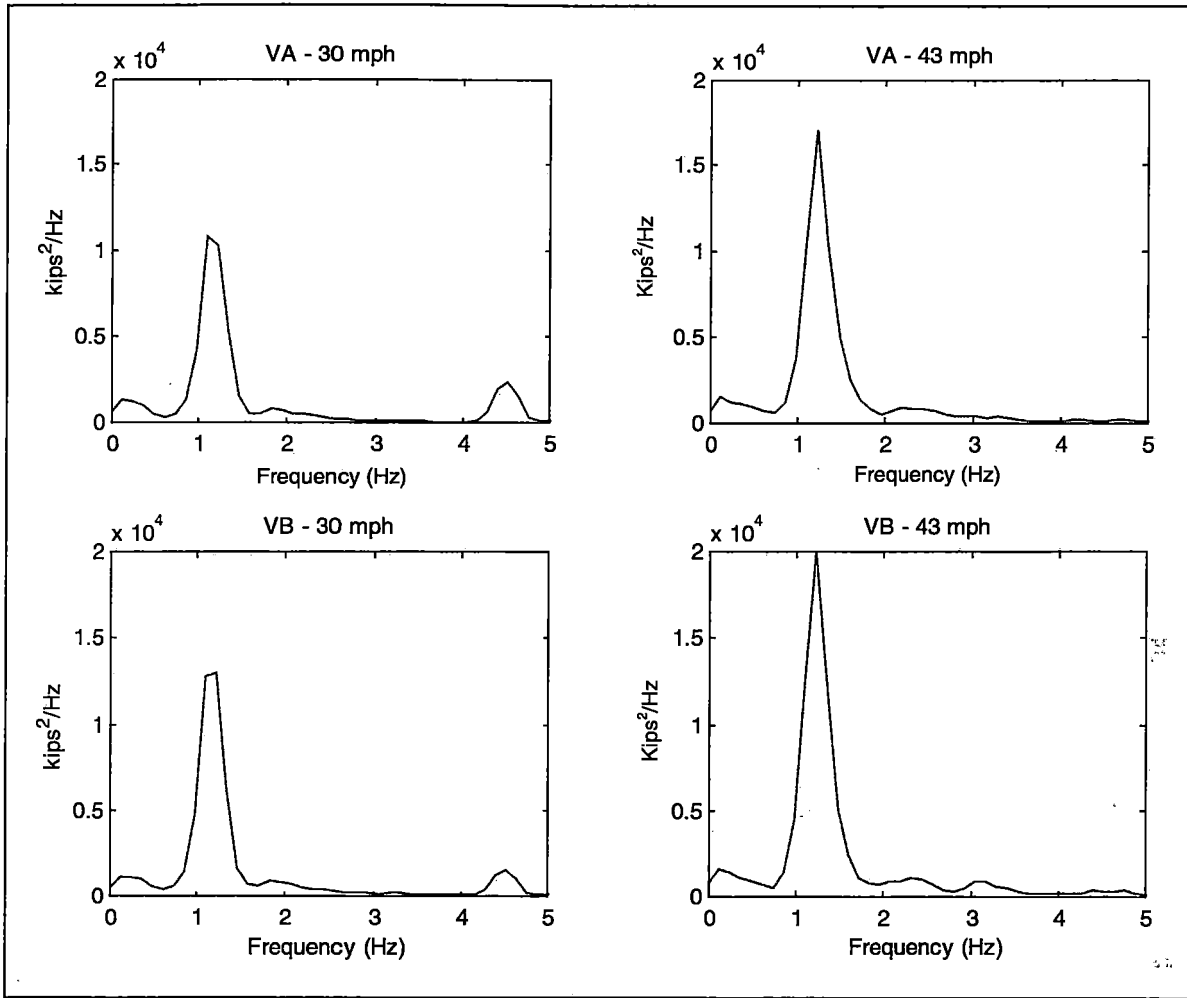


Figure 15. Frequency Contents of Vertical Forces under 125-ton Car at Two Speeds

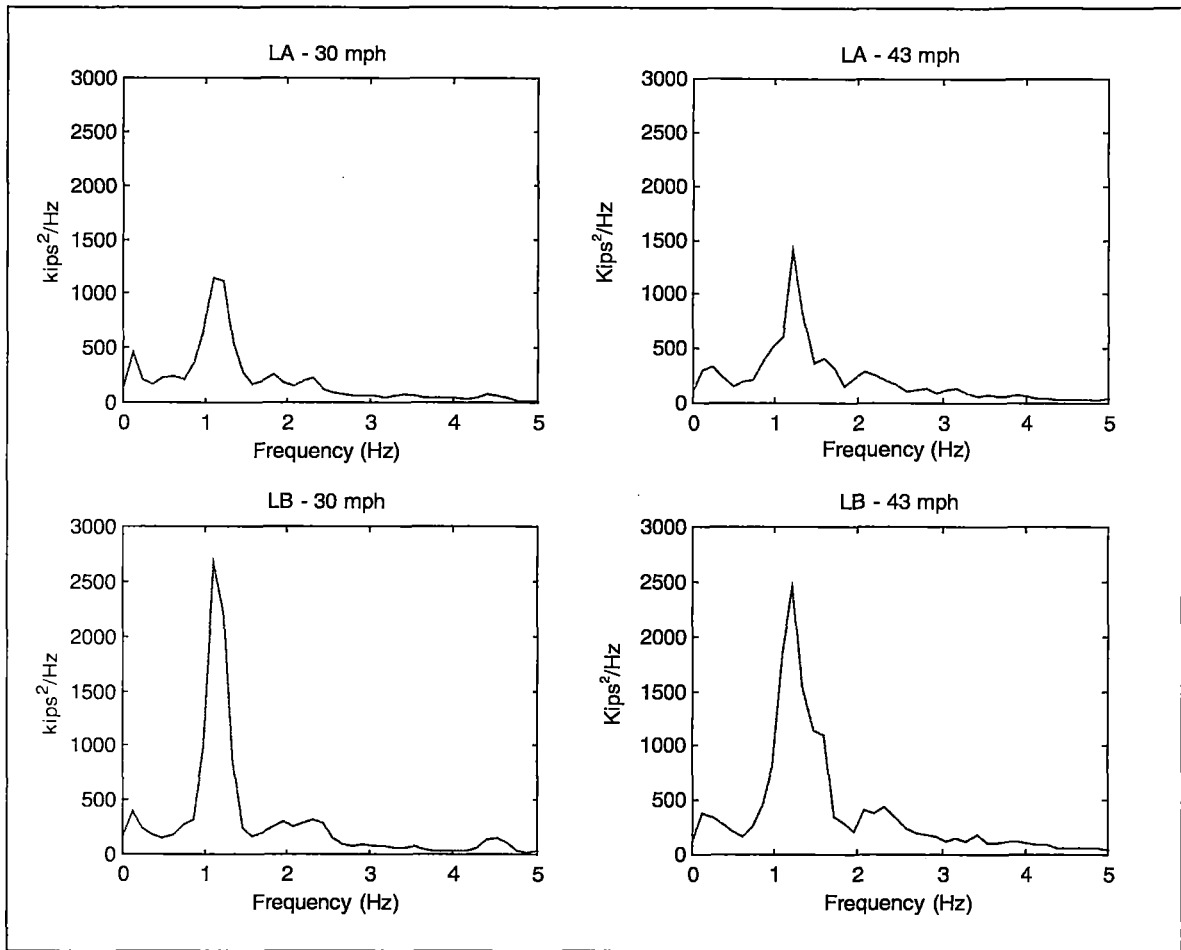


Figure 16. Frequency Contents of Lateral Forces under 125-ton Car at Two Speeds,

Track Geometry (Space Curves) Data

Figures 17 and 18 show the PSD results for the track geometry in the vertical and lateral directions. As shown, at 30 mph, geometry deviations mainly occurred in wide bands approximately from 0.3 to 1.5 Hz, which were related to geometry deviations at various wavelengths. However, the major wavelength of those deviations appeared to be 80 ft (or 0.6 Hz). At 43 mph, geometry deviations (lateral and vertical) mainly occurred at a band from 0.4 to 2 Hz, which corresponded to similar wavelengths measured at 30 mph.

In fact, the HTL consisted of rails welded or jointed at different lengths. But 39- to 80-foot rails are the most common. The joints or welds for those rails most likely contributed to the major frequency bands in the PSD results shown in Figures 17 and 18.

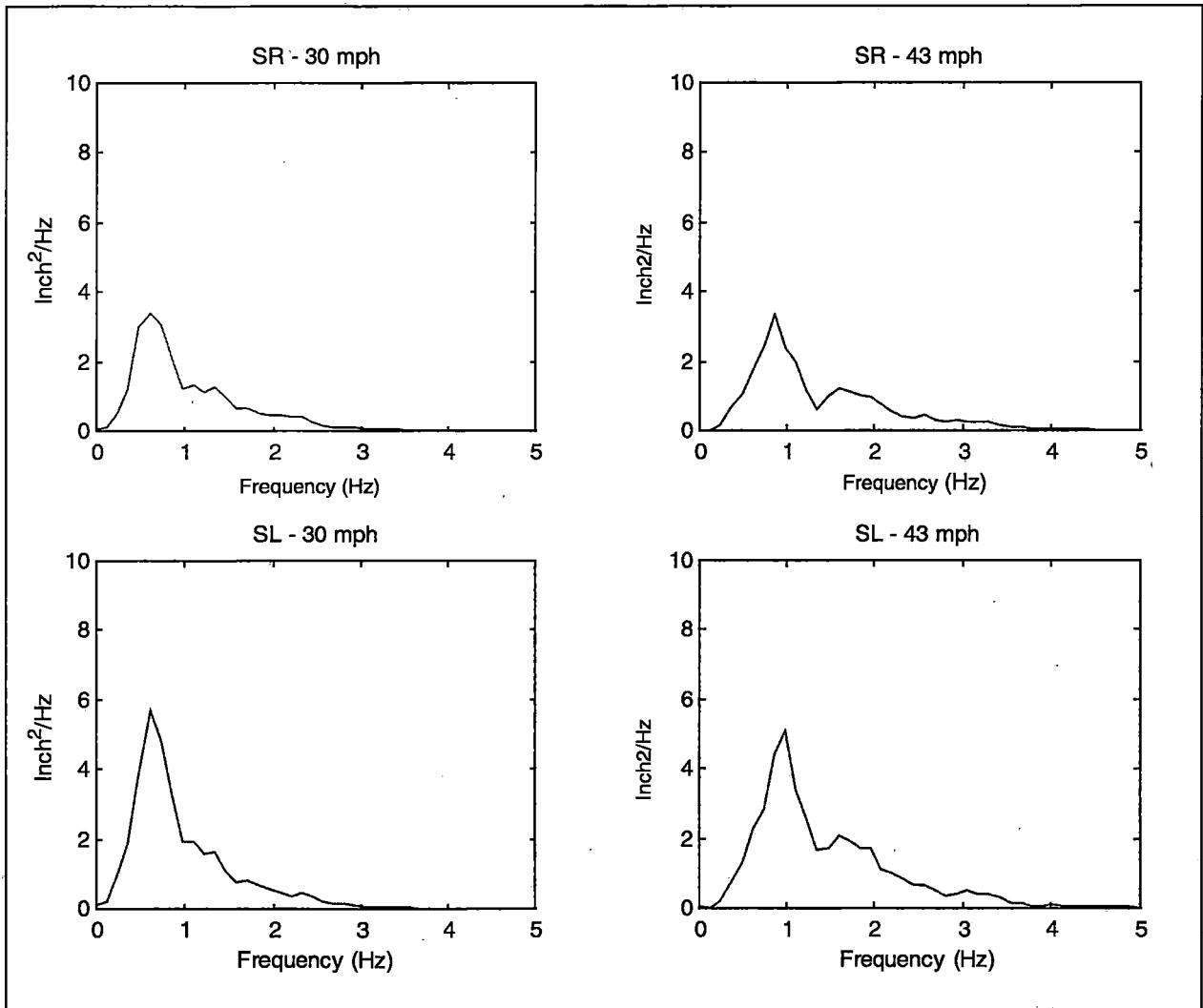


Figure 17. Frequency Contents of Vertical Geometry Results (Space Curves) Measured at Two Speeds,

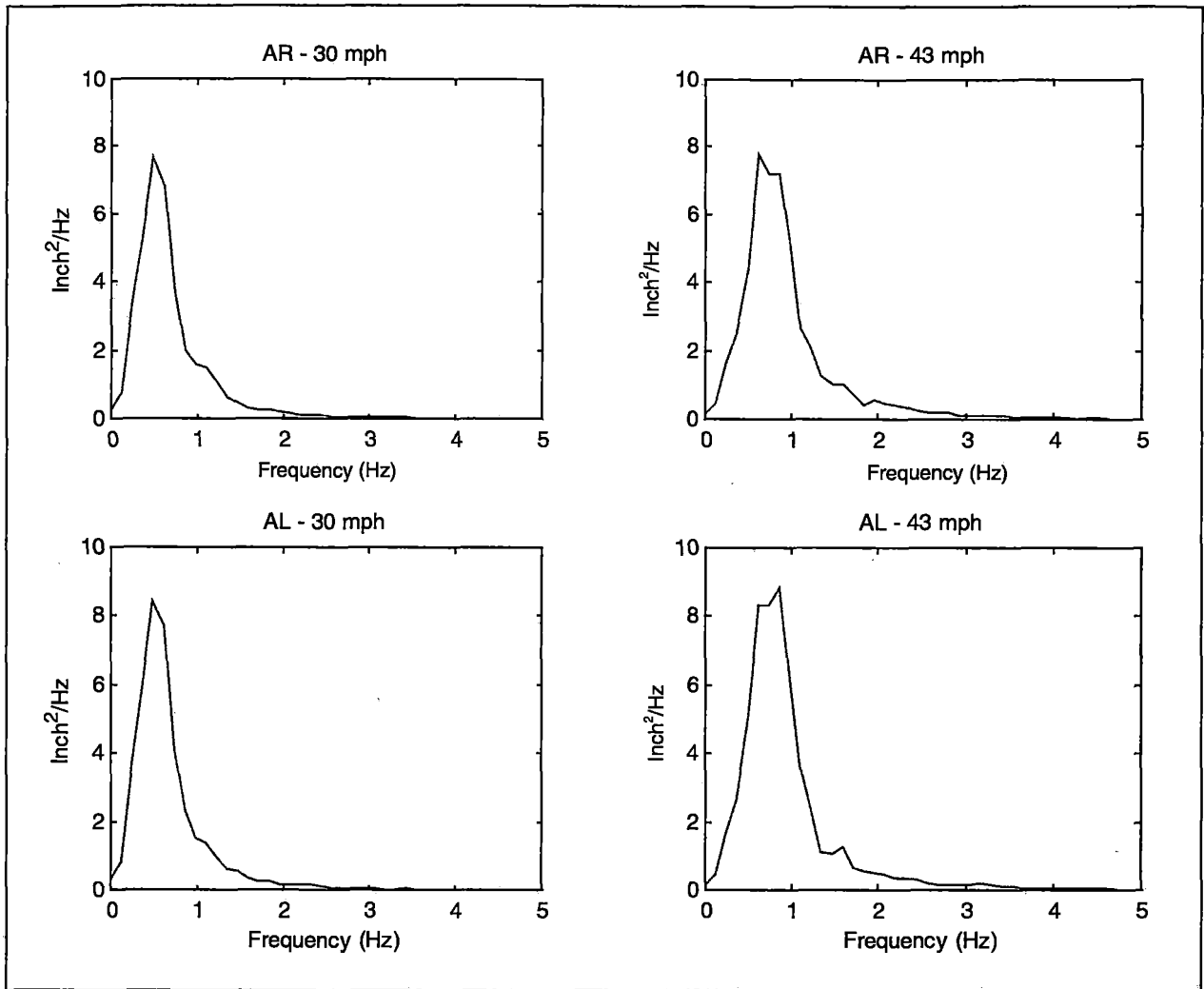


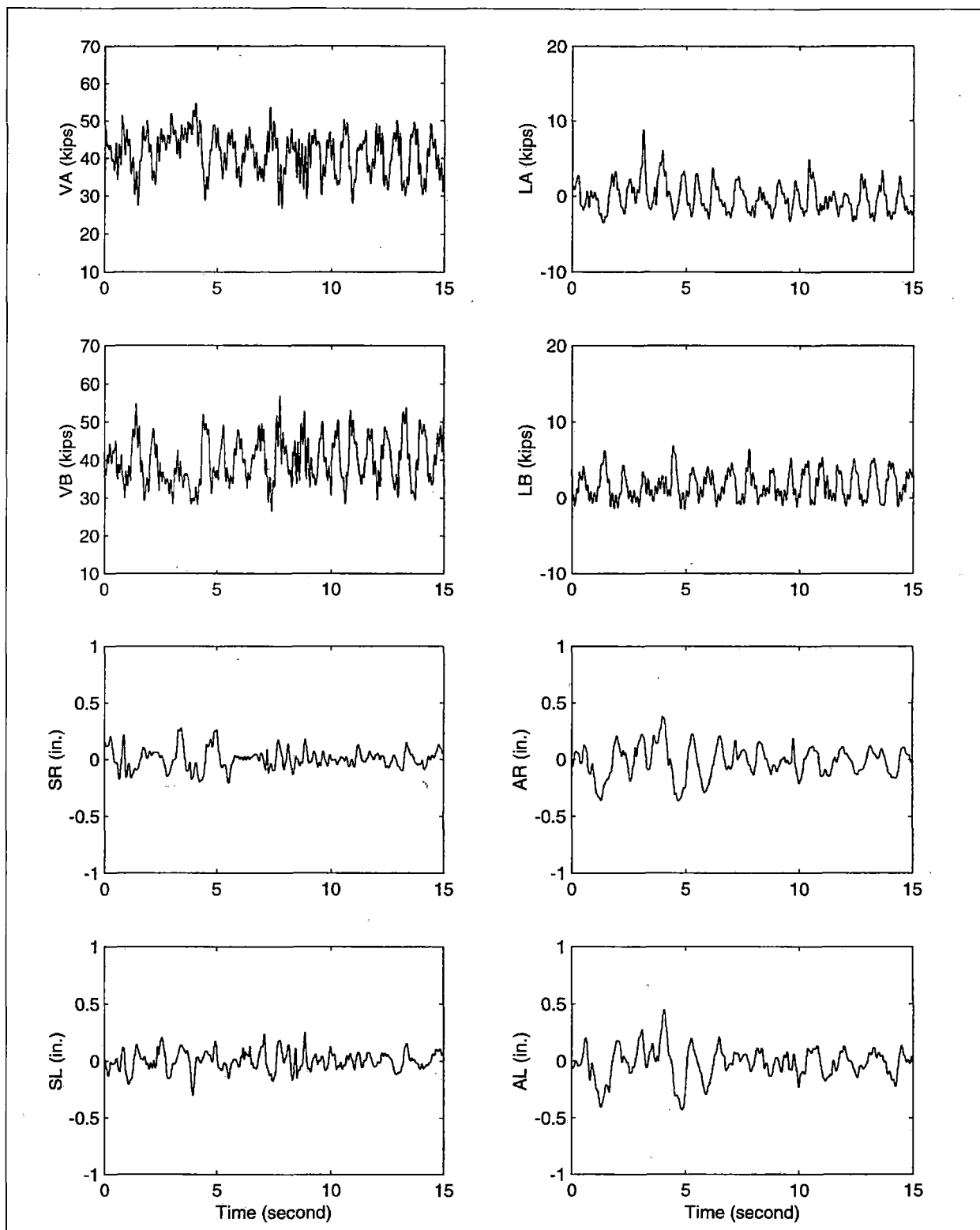
Figure 18. Frequency Contents of Track Geometry (Space Curves) Measured at Two Speeds,

A comparison between Figures 17 and 18 shows that the magnitudes of PSD results at the major peaks were higher in the lateral direction than in the vertical direction. This indicates more irregular geometry conditions in the lateral direction than in the vertical direction for the HTL.

Overall, at 30 to 43 mph, track geometry (space curves) showed major geometry deviations at frequencies ranging from 0.3 to 2.0 Hz. These deviations provided the excitations to generate dynamic vehicle responses at the resonant frequency shown in Figures 15 and 16. The resonant frequency of 1.1-1.2 Hz is well within the range of frequencies shown in Figures 17 and 18.

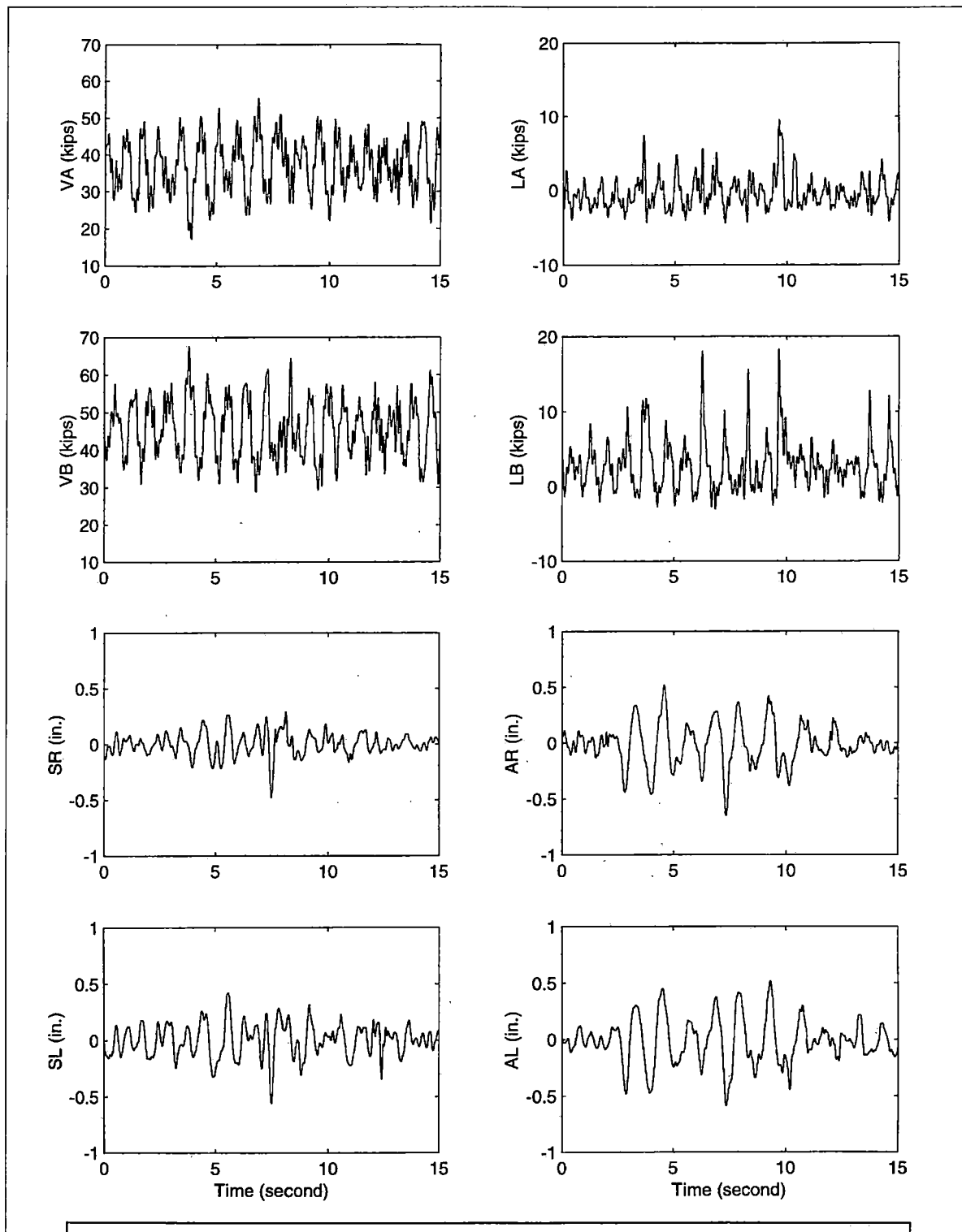
Wave Forms of Wheel Loads and Track Geometry (Space Curves) Data

The typical wave forms of wheel loads and track geometry data, obtained at 43 mph, are given in Figures 19 and 20 for a portion of tangent section (Section 33) and a portion of curve section (Section 3 – 5 degree). As shown, whether vertical or lateral, wheel loads between the two rails (wheel A – inside rail, wheel B – outside rail) were mostly anti-phase (characteristic of lower center roll). The frequency band of track geometry data can be seen to be wider and more complicated than that of wheel loads. A comparison between the vertical and lateral track geometry data shows that the HTL was more irregular laterally than vertically. In addition, the lateral deviations can be seen to be in-phase between the two rails, which however is not the case for vertical deviations. A comparison between Figures 19 and 20 shows more irregular geometry conditions and higher wheel loads in the curve than in the tangent.



Legend:
 VA, VB, LA, LB = Vertical and lateral forces for A and B wheels, respectively.
 SR, SL, AR, AL = Vertical profiles and lateral alignments for the right and left rails, respectively.

Figure 19. Typical Wave Forms of Wheel Loads and Track Geometry (Space Curves), Tangent



Legend:
 VA, VB, LA, LB = Vertical and lateral forces for A and B wheels, respectively.
 SR, SL, AR, AL = Vertical profiles and lateral alignments for the right and left rails, respectively.

Figure 20. Typical Wave Forms of Wheel Loads and Track Geometry (Space Curves) Data, 5-degree Curve

3.4.2 Coherence Analyses

Coherence analysis is often used to help in determining how well an output parameter (i.e., a vehicle response parameter) is related to an input parameter (i.e., a track geometry parameter). This analysis is performed in frequency domain and gives coherence values ranging from 0 to 1. A coherence value of unity at a specific frequency indicates that the output is directly related to the input at that frequency; whereas, a coherence value of zero indicates no relationship between the input and the output.

Only ordinary coherence analysis was done in this study. In this analysis, coherence values were determined only for a single input parameter to a single output parameter. Input parameters were four space curves (alignment left, AL, and right AR, surface left, SL, and right, SR), and output parameters were two wheel loads on the outside rail (vertical load, VB, and lateral load, LB). In addition, several combinations of track space curves (e.g., the difference between surface left and right being equivalent to cross level) were also considered as input parameters.

It must be noted that coherence analysis is based on a linear system assumption. Therefore, any nonlinear behavior in the vehicle/track system will have influence on the results.

The following coherence results were determined using the test run conducted at 43 mph in a clockwise direction over the entire HTL including the bypass. Because the major frequency contents of wheel loads and track geometry obtained at this speed (Figures 15 to 18) were significant only up to 5 Hz, the following coherence results are given only up to 5 Hz as well.

Figures 21 and 22 show the coherence results between single geometry parameter inputs to single wheel load outputs for the test vehicle. In general, the coherence values were low for all the single input to output cases. This indicates that any wheel load was not closely related to any single geometry parameter.

However, vertical and lateral wheel loads can be seen to be more related to alignment deviations. As shown in Figure 21, to a certain extent (a coherence value at roughly 0.5), wheel loads can be seen to be related to alignment deviation at about 1 Hz, which is close to major dynamic vehicle response at its resonant frequency (1.1 to 1.2 Hz). However, at this frequency, the wheel loads were poorly related to vertical deviations on the HTL (Figure 22). In other words, the alignment deviations on the HTL contributed more to the dynamic action of the 125-ton test car.

Several combinations of track geometry (space curves) data were used as inputs. These combinations were the averages and the differences between two sets of track geometry data as well as between two sets of vertical track geometry data. It was found that except for an equivalent cross level parameter (i.e., the difference between two vertical surfaces), use of other space curve combinations as inputs did not lead to more direct relationships to wheel load outputs.

However, within the frequency range from 0.5 to 2 Hz, a cross level parameter was found to be more related to wheel load outputs than any vertical surface parameter. Figure 23 shows coherence results between an equivalent cross level input to wheel load outputs. Although the coherence values are still not high, the wheel loads are shown to be more related to cross level than any single vertical surface parameter shown in Figure 22.

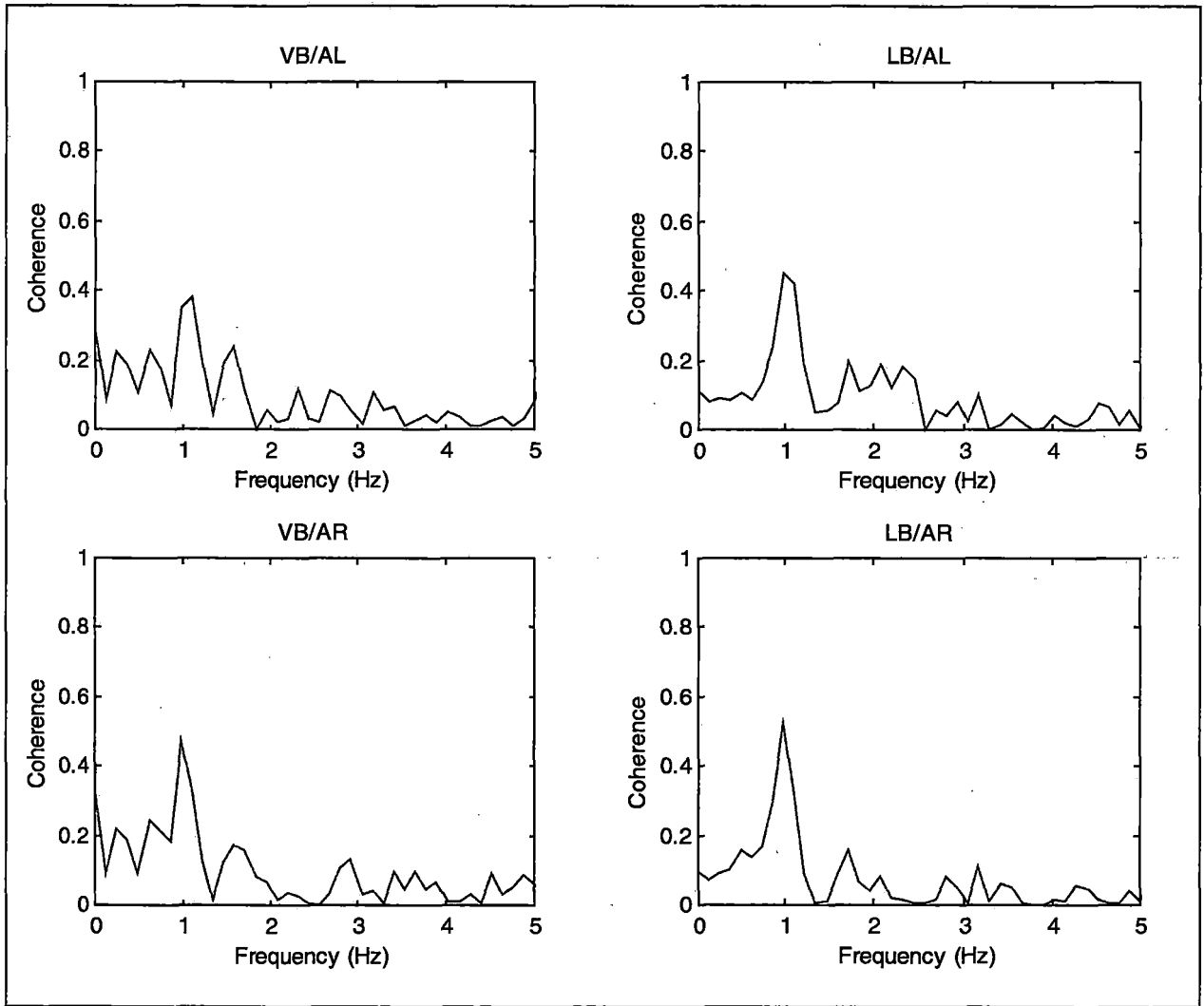


Figure 21. Coherence Results between Lateral Track Geometry (Space Curves) and Test Wheel Loads

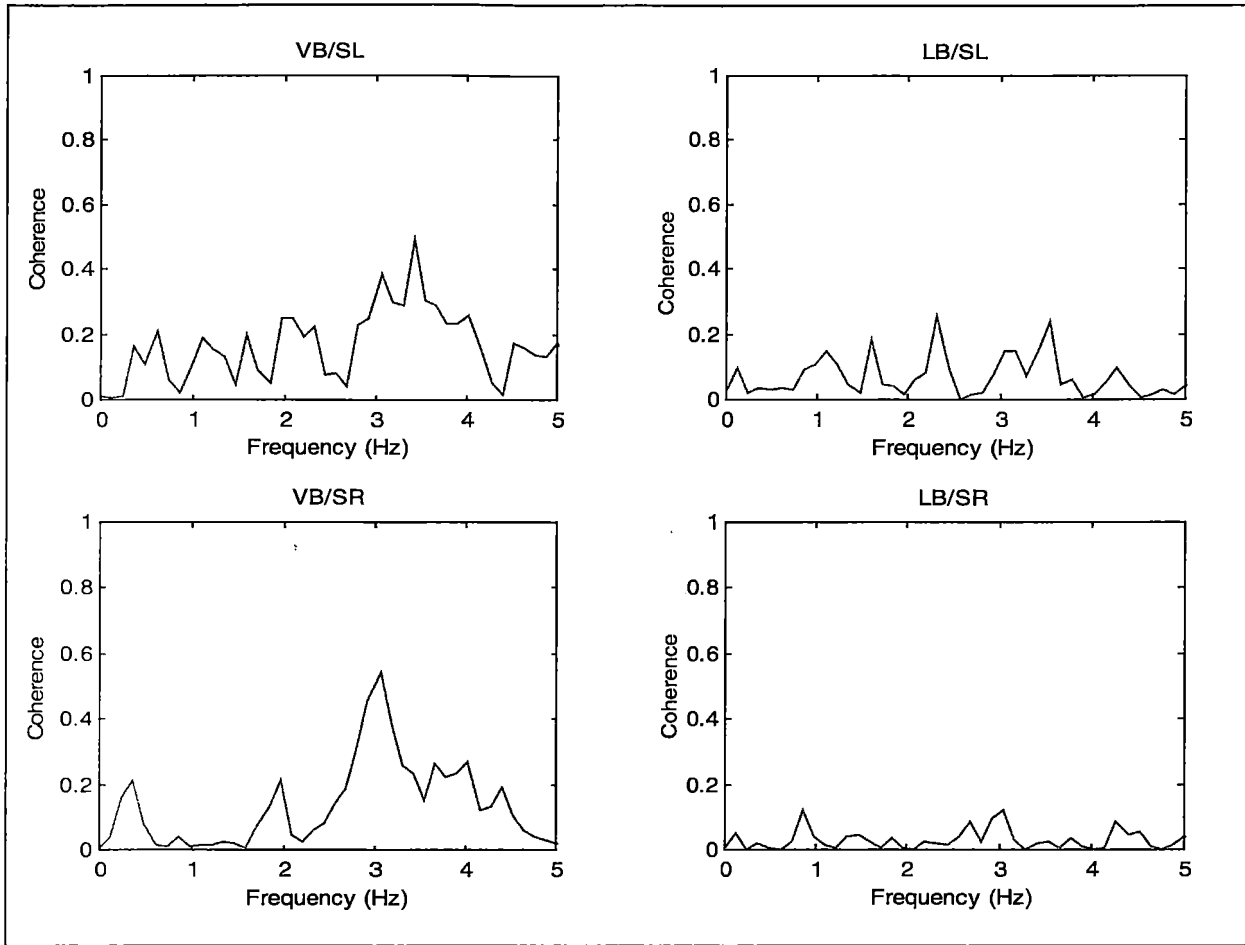


Figure 22. Coherence Results between Vertical Geometry (Space Curves) Data and 125-ton Wheel Loads on High Rail

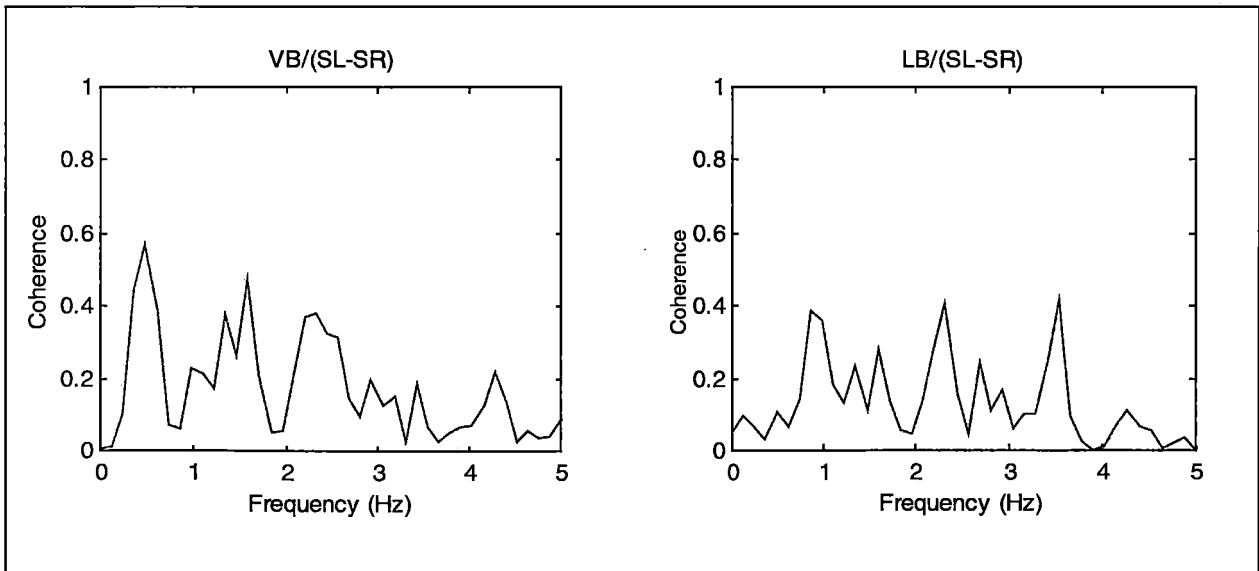


Figure 23. Coherence Results between Cross Level and 125-ton Wheel Loads on High Rail

3.4.3 Running Standard Deviations

Figures 24 to 25 show the track geometry and the corresponding HAL wheel loads. These results were obtained from the run at 43 mph. The test consist ran in a clockwise direction and along the loop including the bypass track. In each figure, two results are shown. The lighter shaded line is the time history of a measured parameter (a space-curve parameter or a wheel load). The dark line is the “running standard deviation.”

The running standard deviation (STD) is calculated from the time history: a standard deviation value is determined from a 100-foot window of the time history, and it gives an indication of the variation within this window. As this window is moved forward (for each move dropping one measurement point at the beginning and adding one point at the end), a profile of standard deviation (i.e., running standard deviation) can then be obtained for the entire time history.

Running standard deviation can give a better visual manifestation of variation throughout a long stretch of track.³ This is illustrated in the comparisons between the time histories and the running standard deviations shown in Figures 24 and 25. Magnitudes of standard deviation for any 100-foot windows are associated with dynamic variations of wheel forces or deviations of geometry conditions.

For example, two characteristics of geometry variations can be described using running standard deviation on geometry data: they are roughness at specific spots and variation for a stretch of track. A “rougher” spot will correspond to a higher value of standard deviation, and a “more variable” section will have a more variable profile of standard deviation.

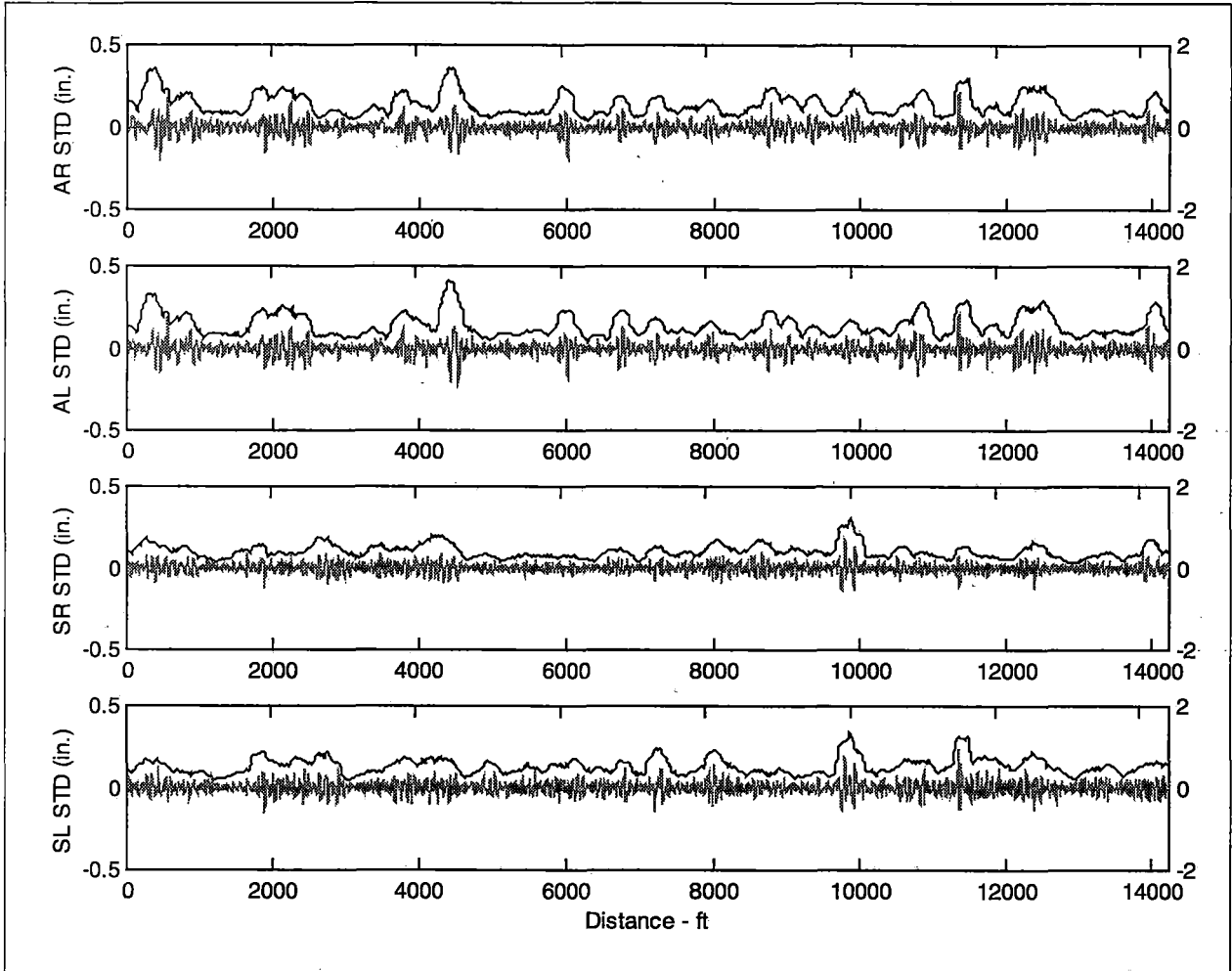
Track geometry space curves data

Figure 24 gives the track geometry data and their running standard deviations for the entire HTL loop. Three trends can be observed in these results. The first trend is that the lateral geometry variations (AL and AR) are much more consistent between the two rails than the vertical geometry variations (SL and SR) on the HTL. Higher lateral

deviations (misalignments) measured on one rail were consistently matched by the higher deviations measured on the other rail.

The second trend is that the HTL track had higher irregularities and more variability in the lateral direction than in the vertical direction. For many locations, the running standard deviations were higher for lateral geometry than for vertical geometry. Furthermore, throughout the HTL, the standard deviation values for lateral geometry were more variable than for vertical geometry. These differences in geometry conditions between lateral and vertical directions seem reasonable given that the HTL track configuration consists of many curves and spirals but has, on the other hand, very firm substructure support.

The third trend is that although higher lateral and vertical geometry deviations on the HTL did not always occur simultaneously at the same locations, vertical track geometry was relatively irregular in those places where lateral track geometry was irregular. In other words, higher irregularity in lateral direction was mostly likely accompanied by the higher irregularity in vertical direction.

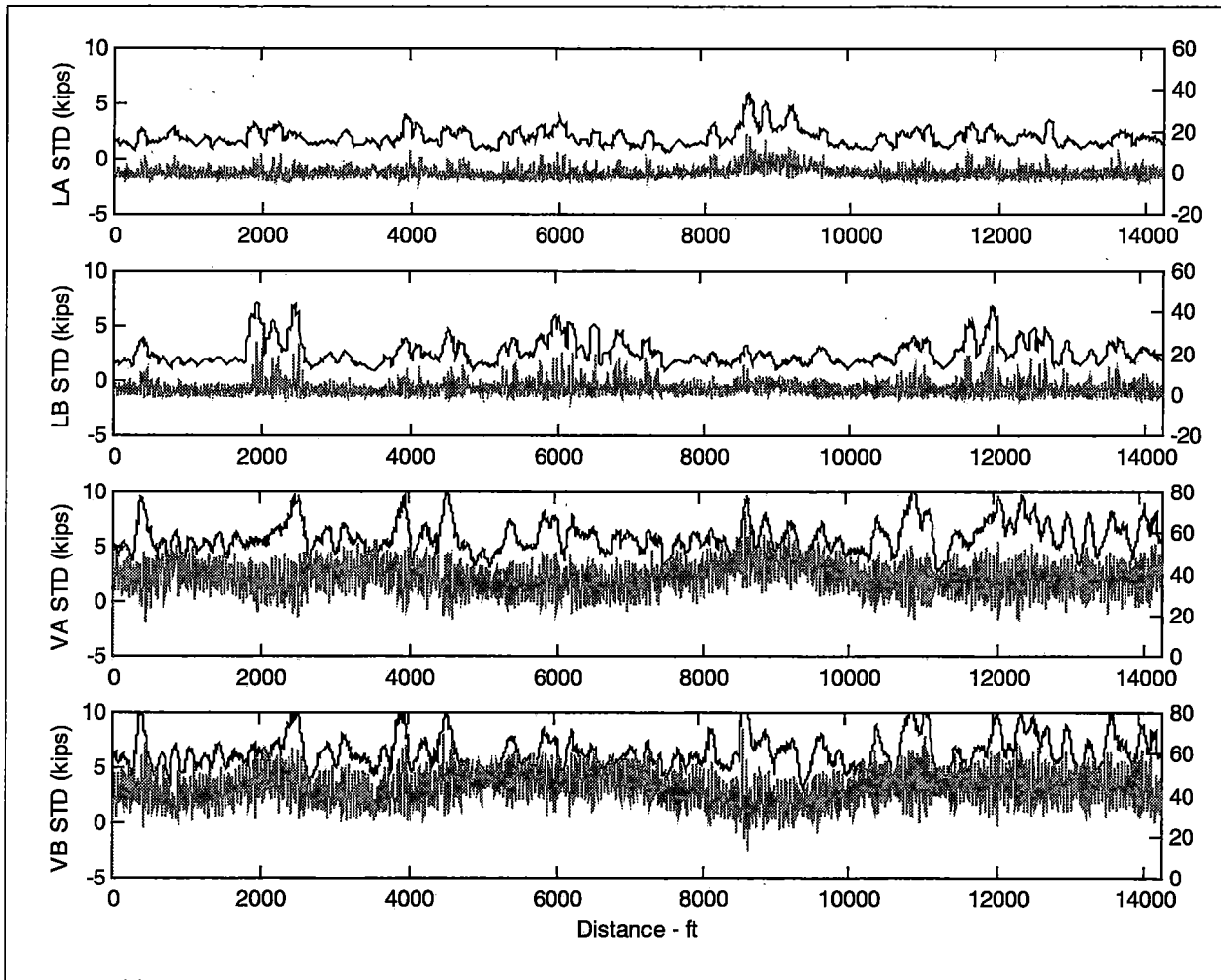


Legend:

VA, VB, LA, LB = Vertical and lateral forces for A and B wheels, respectively.

SR, SL, AR, AL= Vertical profiles and lateral alignments for the right and left rails, respectively.

Figure 24. Running Standard Deviation Results Overlaying RawTrack Geometry (Space Curves) Data



Legend:
 VA, VB, LA, LB = Vertical and lateral forces for A and B wheels, respectively.
 SR, SL, AR, AL = Vertical profiles and lateral alignments for the right and left rails, respectively.

Figure 25. Running Standard Deviation Results Overlaying Raw Data of HAL Wheel Loads

Wheel loads versus geometry:

Figure 25 shows the time histories and the corresponding running standard deviations of the wheel loads for the 125-ton test car. Again, magnitudes and variations of standard deviation, as represented by its running values, are used to characterize dynamic variations of wheel loads at specific locations as well as over the entire HTL loop.

As can be seen in Figure 25, dynamic variations of vertical wheel loads were just as significant as those of lateral wheel loads, although the HTL showed higher lateral geometry deviations than vertical deviation (Figure 24). Furthermore, unlike lateral geometry results, which showed consistent deviations between the two rails, dynamic variations of lateral wheel loads were not consistent between the two rails. Instead, at 43 mph, the outside rail (wheel B) experienced more variations than the inside rail (wheel A). These results showed again that any measured dynamic wheel load was a response to the excitation of combined geometry deviations between the two rails, in both the lateral and vertical directions.

A comparison between track geometry (Figure 24) and wheel loads (Figure 25) shows a more distinct dependence of wheel loads on lateral geometry deviations. For example, the locations at roughly 2,000 ft, 4,000 ft, 6,000 ft, 12,000 ft, where higher dynamic wheel loads can be seen, also showed higher track roughness in lateral directions. The dependence of wheel load variations on vertical geometry variations is not as obvious. For example, the one vertically rough spots at 10,000 feet does not correspond with higher variations of lateral and vertical loads.

3.5 HTL GEOMETRY DEVELOPMENT AS FUNCTION OF TRAFFIC

The regular track geometry inspection by the EM80 produced geometry measurement records as a function of HAL traffic on the HTL. These records include lateral alignments and vertical profiles based on a 62-foot chord length, gage deviations, and cross level results, at various tonnage levels.

Figure 26 gives examples of geometry development as a function of traffic for several major HTL sections. Shown in this figure are modified standard deviation values of the two geometry parameters for Section 5 (tangent section including the bridge), Section 7 (reverse 5-degree curve), Section 25 (6-degree curve), and Section 29 (tangent low track modulus section reinforced with Geoweb). The modified standard values are 2.58 times standard deviations of each geometry parameter for each section. Based on a normal distribution assumption of geometry deviations for each section, these modified standard deviation values are the deviation magnitudes inclusive of 99 percent of the measured data. Therefore, these results indicate the development of irregularities as a function of heavy axle load tonnage, as well as give a comparison of the magnitudes of geometry deviation with respect to the FRA track geometry limits.¹ For the class 4 HTL track, the limits are 2 inches for surface and 1.5 inches for alignment.

The geometry developments shown in this figure were obtained for approximately 100 MGT during 1998. As can be seen, for the vertical profiles, Sections 7, 25, and 29 experienced similar geometry variations. Geometry degradations due to traffic for these three sections were insignificant. However, Section 5 had higher geometry irregularities, as evident by its much higher standard deviation values at various MGT levels. In addition, the traffic also appears to have a degrading effect on vertical profiles (Figure 26a). In fact, the higher irregularities for Section 5 were probably caused by the track approaches to the bridge. Over the two approaches, the track was observed to have significant "pumping" movements, probably due to sudden stiffness changes from the regular track foundation to the stiff bridge abutment. The decrease in irregularities in Section 5 following 850 MGT was a result of track surfacing.

Lateral misalignments were more variable among different sections. Section 5, which had higher vertical irregularities, did not exhibit higher lateral irregularities. As shown in Figure 26b, the HAL traffic did not have a significant degrading effect on lateral track geometry parameters.

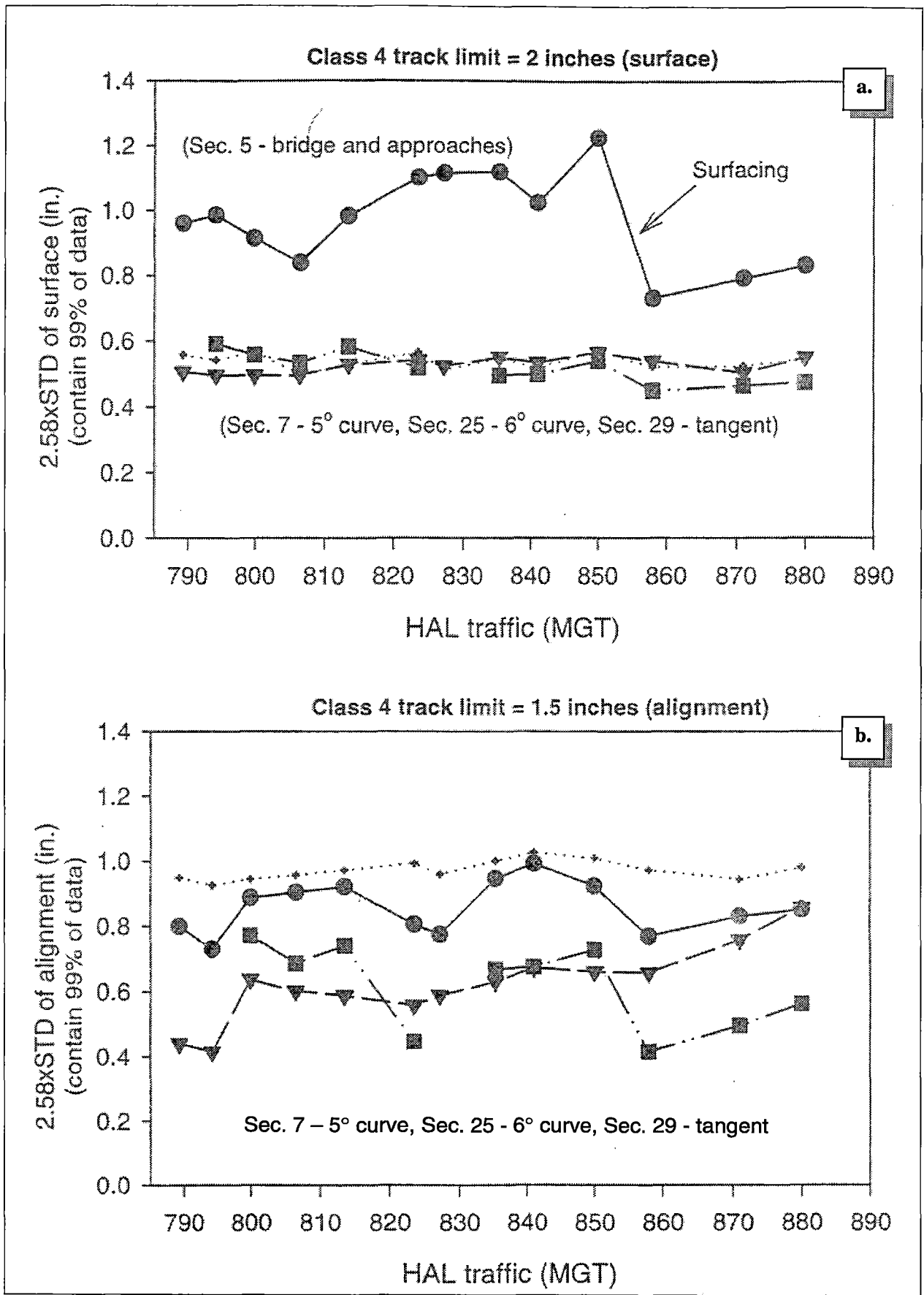


Figure 26. Geometry Development with Traffic for Several HTL Sections

Overall, the track roughness for each of those sections was well within the FRA safety limits, as indicated by the comparison of geometry deviation results with the FRA limits.

4.0 SUMMARY AND CONCLUSIONS

Two vehicle/track interaction tests were conducted on the HTL during late January and early June of 1998, respectively. These tests included measurements of vehicle responses such as wheel loads and car body accelerations. The test vehicles included a 125-ton gondola equipped with improved suspension trucks and a 100-ton covered hopper equipped with standard trucks. Track geometry conditions were recorded using the new AAR system based on the inertial/laser technology. The following sections draw the main conclusions from these two tests.

4.1 125-TON WHEEL LOADS

Vertical wheel loads were generated mainly between 20 and 60 kips under nominal FAST train operation with means from 35 to 45 kips for various HTL sections. Lateral wheel loads were mainly between -5 (gage direction) and +15 kips (field direction) with means being -1 to +7 kips for various HTL sections. In curves, lateral wheel loads on both rails were primarily in the field direction indicating lateral vehicle/track interaction in a gage-widening mode.

On the HTL, dynamic wheel loads generated by the 125-ton test car generally resulted from the lower center roll of the car body. At 40 mph, large dynamic vertical loads generated by the 125-ton car (63 to 79 kips) than those (60 to 73 kips) generated by the 100-ton car. This was attributed to the use of the primary suspension pads under the 125-ton trucks, which might have attenuated higher frequency dynamic force components.

Use of the improved suspension trucks under the 125-ton car led to better steering in the curves (decreased angles of attack), which in turn led to significantly lower gage-widening loads. For the entire loop, the 125-ton mean lateral force was 5 kips lower

than that generated by the 100-ton car equipped with the standard trucks. In the 6-degree curve, the 125-ton mean lateral force was 8 kips lower.

In curves, net lateral axle load increased as speed deviated from the balance speed. As speed changed, redistribution of the car weight was not the only reason for the changing lateral wheel loads on the two rails. The axle (truck) steered better when the operation speed was closer to the balance speed, leading to lower net lateral axle loads.

4.2 HTL GEOMETRY CONDITIONS

For close to 100 MGT, the HAL traffic caused insignificant geometry degradations on most of the HTL track sections. However, the bridge section exhibited higher vertical irregularities. The higher vertical irregularities mainly occurred over the bridge approaches, where track vertical movements (pumping) were observed. Rapid track stiffness variation typical of transition zones such as bridge approaches might have caused the “pumping” action in the approaches.

On the HTL, lateral geometry variations were mostly in-phase between the two rails. However, this was not the case for vertical geometry variations. Higher lateral geometry deviations (misalignments) measured on one rail were consistently matched by the higher deviations measured on the opposite rail. In addition, the HTL was more variable in the lateral direction than in the vertical direction.

4.3 125-TON VEHICLE RESPONSE VERSUS TRACK GEOMETRY CONDITION

The tests with two different vehicles indicated that over the same track geometry conditions, vehicles with different suspension and stiffness characteristics would respond differently. Therefore, relationships between vehicle responses and track geometry conditions are vehicle dependent.

Although the HTL showed higher lateral geometry deviations than vertical deviations, dynamic variations in vertical wheel loads were just as significant as dynamic *variations* in lateral wheel loads. Furthermore, unlike geometry results, which showed consistent lateral deviations between the two rails, dynamic variations in lateral

wheel loads were not consistent between the two rails. Instead, at 43 mph, the outside rail experienced more variations than the inside rail. In other words, any measured dynamic wheel load was a response to the excitation of combined geometry deviations between the two rails, in both the lateral and vertical directions.

The coherence value, that defines the relationship between two signals, was generally low for all cases relating a single geometry parameter such as input to a single wheel load as output. This also indicates that any wheel load was not directly related to any single geometry parameter. Vertical and lateral wheel loads were found to be more related to alignment deviations, or the vehicles responded more to alignment deviations. Use of a cross level parameter (difference of the two vertical profiles) improved coherence values as compared to any single vertical profile, indicating that wheel load variations were more related to the cross level parameter than to a single surface parameter.

Acknowledgment

The AAR and FRA jointly funded this project under the FAST/HAL research program. Dr. Magdy El-Sibaie, Chief of FRA Track Research Division, initiated this study. His support is greatly appreciated. The following TTCI personnel, Messrs. Semih Kalay, Bill Shust, and Curtis Urban provided guidance and advice. Their contributions are gratefully acknowledged.

References

1. Federal Railroad Administration *Manual of Track Safety Standards*, 1998.
2. Klauser, P., Florom, R., and Urban, C. "On-track Test Results for the Heavy Axle Load Alternative Suspension Project," Report R-896, Association of American Railroads, September 1996.
3. Ebersohn, W. "Substructure Influence on Track Maintenance Requirements," Ph.D. dissertation, Department of Civil Engineering, University of Massachusetts, Amherst, 1995.

Vehicle/Track Interaction Tests On The Heavy Tonnage Loop, D. Li,
L. Smith, 1999 -02-Track-Train Dynamics

SMEAD CO VP58SA



**Transportation
Technology Center, Inc.**

**55500 DOT Road
P.O. Box 11130
Pueblo, Colorado 81001-0130 USA**

A SUBSIDIARY OF THE ASSOCIATION OF AMERICAN RAILROADS

